P-TYPE SEMICONDUCTOR SENSITIZED SOLAR CELLS

FATEMEH SAFARI ALAMUTI

A THESIS SUBMITTED

FOR THE DEGREE OF MASTER OF ENGINEERING

DEPARTMENT OF CHEMICAL AND BIOMOLECULAR ENGINEERING

NATIONAL UNIVERSITY OF SINGAPORE

2014

Declaration

I hereby declare that this thesis is my original work and it has been written by me in its entirety. I have duly acknowledged all the sources of information which have been used in the thesis. This thesis has also not been submitted for any degree in any university previously.

Fatemeh Safari Alamuti
26/06/2014

Acknowledgement

I would like to express my sincere gratitude to my supervisor, A/P Lin Yue Lanry Yung for his supports and invaluable advices throughout my study at NUS.

I will also take this opportunity to express my utmost thanks to Dr. Wang Qing for giving me the opportunity to work in his lab and under his supervision in Nano core institute of NUS.

My warmest thanks also go to my lab mates and colleagues in chemical and bimolecular and Material Science and Engineering departments for their technical supports and advises.

Finally, my heartiest appreciation is to my husband for his help and support throughout my study and research which make it possible for me to do this work.

Table of Contents

Summary

Semiconductor sensitized solar cell (SSC) is one of the latest generations of PVs in which photogenerated charge carriers are separated into two different materials. The inorganic semiconductor, as the sensitizer offers exciting opto-electronic properties and tunable band gap. As yet, most of the SSCs have been fabricated based on the photoanode cell using n-type semiconductor materials.

Sensitization of p-type semiconductor materials such as NiO with semiconductor sensitizers such as CdSe which is the target of this research is a very novel method which could open up a new vista toward the new generation of solar cells. In this research, attempts to synthesize NiO film, fabrication of p-NiO-SSC, photovoltaic performance improvement and diffusion length measurement are targeted and promising IPCE have been achieved. With a polysulfide redox electrolyte and a Pt counter electrode, CdX (X=S and Se)-sensitized p-NiO solar cells operating in a photocathodic mode are unambiguously demonstrated when NiO blocking layers are used, which are critical to prevent anodic photocurrent due to electron injection from CdX into the SnO_2:F substrate. To decrease the recombination rate, CdS barrier layer was deposited between NiO and CdSe sensitizer which results in much enhanced cell performance. Front and rear spectral incident photon-to-current efficiency (IPCE) measurements were used to investigate charge collection and separation in the cells. The measurements indicate that charge collection in this system is limited by a short hole diffusion length. Furthermore, the effect of surface engineering and the heterojunction interface formation on the enhancement of NiO-SSC performance has been systematically scrutinized. It was observed that the surface engineering enhanced the performance and IPCE of solar cell. Specifically, existence of ZnSe layer resulted

in two fold IPCE enhancement in the case of ZnSe/CdS-NiO. In addition, comparison of CdS/CdSe-NiO and ZnS/CdSe-NiO revealed that the less lattice mismatch between the sensitizer and barrier layer gives rise to a much enhanced performance.

List of tables

List of figures

1- Introduction

1.1 Background

Electricity demand is predicted to grow at an annual rate of about 3.5%. [1] Conventional carbon-based resources are estimated to be insufficient to meet the requirements and alternative energy resources must be provided. Solar energy is believed to be the best potential alternative as the sun provides 10000 times more energy than the global energy consumption. [1] Photovoltaic cell (PV) is the most common approach to generate an electrical power from the solar radiation. In addition to the potential for the sufficient energy supply, PV effectively contributes to significant reduction of greenhouse gas. Generally, photovoltaic cells are classified into three generations. Conventional Silicon solar cells are first-generation PVs.[2] The requirements for high-quality materials and high production cost of this type, led to the development of second generation PVs or so-called thin film solar cells. The main motivation to develop thin film solar cells was to fabricate a cost-effective device with moderate efficiency.[2] Although both first and second generations have paved the way toward commercialization, the current PV systems cannot compete with alternative carbon based energy resources. Thus, intensive researches are essential for further improving the power conversion efficiency and lowering the cost. Furthermore, the maximum efficiency of these cells is thermodynamically limited to 33% which is also known as Shockley–Queisser limit.[3]

Recognizing the constrains, scientists later established the concepts of third generation of PVs to reach conversion efficiencies beyond the Shockley–Queisser limit. This generation includes

broad types of solar cells such as multi-junction cells, dye sensitized cells, optical up- and down converters, multiple carrier generation by impact ionization and etc.[2]

Dye sensitized solar cell (DSC) is photoelectrochemical cell in which photogenerated charge carriers are separated into two different material.[2] In the conventional scheme, molecular dye acts as a light absorber; injecting electron into a semiconductor material. While DSC is fairly matured, several strategies have been proposed to further improve the cell performance. One approach is to replace a dye molecule with semiconductor sensitizer (QDs) to form semiconductor sensitized cell (SSC). Besides the cheap and simple synthesis method, semiconductor sensitizer offers exciting opto-electronic properties such as tunable band gap and possibility to manipulate injection and recombination processes, high extinction coefficients and improved light absorption properties, impact ionization effect and multiple carrier generation.[4]

As yet, most of the DSCs and SSCs have been fabricated based on the photoanode cell using n-type semiconductor materials.[3] Recently, solar cells based on the sensitization of p-type semiconductors have attracted much interest. Sensitization of p-type semiconductor materials such as NiO with semiconductor sensitizers such as CdSe which is the target of this thesis is a very novel method which could open up a new vista toward the new generation of solar cells.

1.2 Objectives

This work aims to investigate the p-type based semiconductor sensitized solar cell from proof of concept to the device performance improvements. In this project, firstly, mesoscopic NiO film is synthesized and micron-thick film has been produced by screen-printing method. Secondly, semiconductor-sensitized NiO photocathodes have been fabricated by successive ionic-layer adsorption and reaction (SILAR) deposition of sensitizers including CdS, CdSe and cascaded CdS/CdSe onto mesoscopic NiO films. Then, Detailed morphological, structural and optical properties are characterized to examine the factor determining the photocathode properties. Lastly, the solar cell is fabricated and factors imposing the cell performance are determine. to characterize the solar cell photophysical details hole diffusion length measurement are described. Moreover, in the present study, the effect of surface engineering and the heterojunction interface formation on the enhancement of NiO-SSC performance has been systematically scrutinized.

2- Literature Review

P-type nickel oxide photocathode based solar cells have recently attracted significant interest as a new type of photoelectrochemical cell. **[1, 5]**

Sensitization of p-type semiconductor materials and mainly NiO as well as study of hole injection phenomena have been reported far ago while all were limited to a simple photocathode and not real solar cell. The first report of p-type based solar cell was in 1999 by *Lindquist et. al.* based on dye sensitization of porous NiO film. They achieved a very low efficiency of 0.007% and maximum IPCE of 3.4%. [1] Since then, results of several studies elucidated that the low efficiency of p-type NiO-based DSC stem from several factors. Firstly, NiO-DSC exhibits low V_{oc} which is a result of small potential difference between the quasi-Fermi level of NiO and the redox potential of conventional Iodine/Iodide electrolyte as well as drastic recombination and specifically very fast recombination of the photoinjected holes with reduced dye.[2, 6] Secondly, low j_{sc} caused by poor dye loading, impaired light absorption and thus inefficient hole injection, declines the efficiency.[6, 7] Moreover, studies have shown that the hole diffusion coefficient of NiO film is in the order of ~10^{-8}-10^{-7} cm^2/s which is two orders of magnitude less that electron diffusion coefficient in TiO_2 film. Consequently, the charge collection would be inefficient and results in low efficiency.[7, 8]

In recent years, many efforts have been made to further improve the cell performance[2] These attempts includes synthesis of better quality NiO film[9] replacement of NiO film with other p-type materials [10]designing a dedicated dye molecule [11] and application of new redox mediators [12] such as cobalt complex.

Besides, another approach which has been investigated to overcome existing problems is to use semiconductor nanocrystals (QDs) as sensitizer to replace a dye molecule as QDs sensitizers offer very fascinating properties.[13, 14] Here, we briefly review reported studies.

2.1 The p-type semiconductor film

There are very few metal oxides that display p-type properties, unlike n-type semiconductor where several materials such as TiO_2, ZnO, Nb_2O_5 and SnO_2 have been successfully used.[2]

Nickel oxide is the mostly used p-type material as a photocathode in solar cell due to availability of extensive studies on its properties and fabrication methods.[2]

NiO is a wide band-gap semiconductor (Eg~ 3.60 eV)[15] that exhibit p-type conductivity with good thermal and chemical stabilities. Several methods have been reported in the literature for NiO synthesis including sol-gel method, triblock copolymers template, self-templated method, hydrothermal synthesis, electrodeposition and using commercial NiO nanopowder to make the film.[2]

The mostly used method is so-called sol-gel method in which hydrated nickel precursor (commonly $NiCl_2$) (sol) is used to form nickel dihydroxide (Ni $(OH)_2$) (gel) which is then sintered at 300-500 ^oC.[2] This method has been report by G. Boschloo *et al*.[3] A. Morandeira *et al*.[12] He. *et al* [1]and others.[17,18] This method offers NiO film with mesoporous structure which is desired for solar cell application. However, the main shortcoming of this method is impracticality for making the thick NiO film as the film cracks upon increasing the thickness. Thickest film produced by this method is 2 microns.[2] In 2008 Suzuki *et al.* [16]reported a modified sol-gel method by use of triblock copolymers of polyethylene oxide and polypropylene oxide (PEO-PPO-PEO) as template. Besides the simplicity, this method results in formation of

mesoporous film. Also, it helps to control the particle and pore sizes by applying the co-polymers PEO/PPO and modifying PEO/PPO ratio or by changing Ni precursor to polymer ratio. More importantly, good quality NiO electrode can be fabricated. More recently, modification of Suzuki method resulted in enhanced device performance.[17]

2.2 Sensitizer material

In a p-type DSC upon absorption of light, electron will be excited from HOMO to LUMO level of dye molecule, leaving a hole in HOMO level which will be injected to the valance band of semiconductor film. The sensitizer molecule should possess several properties to be adequate for p-type material.[18] One of the basic requisite is that the sensitizer absorbs in a broad range of wavelength to improve the light harvesting efficiency.[2] Specifically, sensitizer should posses high extension coefficients [4, 6] because mechanical properties of nickel oxide films synthesized so far is very poor and fabrication of high quality thick film is still impossible. As a result, sufficient dye loading is hindered and light harvesting will not be efficient.

Besides, the sensitizer should be photochemically and electrochemically stable and posses more negative reduction potential than that of the mediator to make the regeneration reaction thermodynamically possible.[2]

Several groups have used commercially available Coumarin C343 dye to fabricate NiO-DSC.[1, 6, 9, 19] However, studies show that recombination of generated holes with reduced dye[13,15] plays a major role in cell deficiency. Thus, designing a dedicated dye molecule has been tried by several researchers to enhance the cell efficiency by slowing down the recombination process. *Nattastade* and co workers synthesized the most efficient dye for NiO sensitization so far which

display long-lived charge-separated states. They also attained the highest reported efficiency of 0.3% for NiO-DSC.[11]

2.3 Redox mediator

The redox mediator has two major roles in solar cell: first to regenerate the reduced sensitizers when the hole injected into the valence band of p-type sensitizer and second to transport the electron to the counter electrode to be collected for current generation. [2] Like other parts of the cell, electrolyte also should exhibit specific properties to be adequate. Basically, it should not absorb the light in the region that the sensitizer is active (mainly visible region) and should not be corrosive.[2] In addition, diffusion coefficient of electron should be high to efficiently transport the charge to the counter electrode. More importantly, the redox potential of mediator must be positive than the sensitizer HUMO level and negative that the valance band of semiconductor film.[7]

The most extensively used redox electrolyte for p-DSC is iodide/triiodide electrolyte although it is not optimized for this application.[1, 9, 19] The major disadvantage of this redox molecule is that its redox potential (0.4 V vs. NHE) is very close to the NiO valance band (0.54 V vs. NHE) which limits the maximum achievable Voc.[20]

An alternative electrolyte of cobalt complex has been recently reported[12] and could improve the Voc by 3 orders of magnitude. However, low photocurrent and limitation to the specific dye molecule limits its application.

2.4 Tandem DSCs

Concept of tandem solar cell is one of the major encouraging motivations of photocathode based solar cell improvements.[19] In tandem cell, conventional pt counter electrode is replaced by

photocathode material (mainly sensitized p-NiO) and both photocathode and photoanode (sensitized n-type sensitizer and mainly TiO_2) are implemented to fabricate the cell. The simplified schematic of tandem cell is depicted in Figure 2-1.

Theoretically, the overall photoconversion efficiency of tandem device is higher than n-DSC and it is proved that the maximum theoretical efficiency of tandem cell is 42% compared with 31% in single semiconductor photovoltaic cell.[21] Another aspect of tandem device is that redox mediator does not dictate the photovoltage as photovoltage is the difference between the p-SC valence band potential and the n-SC conduction band potential which propose a potential to achieve higher Voc by choosing proper p-type and n-type materials.[22]

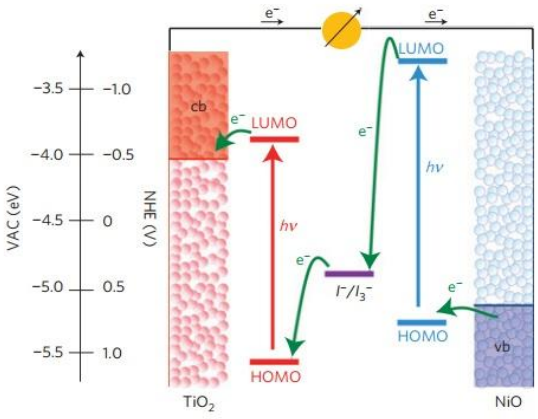

Figure 2-1schematic representation of Tandem solar cell (adopted from reference [2])

Another possibility offered by tandem structure is that it is possible to use different sensitizers with different absorption ranges for each n-type film and p-type film to cover broad range of solar spectrum.[2] Therefore, light harvesting efficiency can be enhanced easily.

First tandem solar cell was reported in 2000 by Lindquist and co-workers which was composed of TiO_2 photoanode and NiO photocathode and increased the Voc 82 mV more than TiO_2 only device. However, the cell efficiency was limited by low current of NiO.[23]

Later, application of better quality NiO film and more efficient dye molecule resulted in the tandem cell with better performance.[24] Furthermore, cobalt complex redox mediator and designed dye implementation resulted in further enhancement and researcher could reach Voc that matches with sum of Voc produced by each photoelectrode**.**[4] Recently, *Natastade* and co-workers published a paper in Nature materials that reported fabrication of tandem cell with superior performance than individual photocathode based or photoanode based device for the first time, elucidating the possibility to enhance cell performance by tandem concept.[11]

2.5 Photocathode based Semiconductor sensitized solar cell

Significant improvements have been made in recent years in p-type DSC. However, the performance of dye-sensitized nanocrystalline NiO solar cells is still far below the TiO_2-DSC counterpart.[2]

Besides modifying the NiO film properties, designing a dye molecules and optimizing the electrolyte, another approach which has been investigated to overcome existing problems is to fabricate semiconductor sensitized cell (SSC) by use of semiconductor nanocrystals (QDs) as sensitizer to replace a dye molecule in p-type cells.[13, 14, 25]

It is very important to note that although the working principle of SSC is very similar to DSC, there are some conceptual differences. In other words, it is not simply replacing the dye molecule sensitizer to semiconductor. It is proposed that the most significant difference between DSC and SSC is the presence of surface states in semiconductor sensitizer [26] and thus surface treatments

to passivate these stats can significantly enhance SSC performance.[27] Other dissimilarities includes electrolyte used as conventional iodide/triiodide cannot be used for SSC because of corrosion problems, low photocatalytic activity of pt counter electrode toward polysulfide electrolyte which is the common electrolyte for SSC and requirement to find ideal counter electrodes, possibilities to use aqueous electrolytes and also wider variety of materials and synthesis method used for semiconductor sensitizer**.**[28]

Semiconductor sensitized solar cells have very exciting and unique properties and attracted significant interests in recent years.[13, 14, 25-28] It is possible to tune the band gap of QDs by varying the particle size due to the quantum confinement effect.[29, 30] As a result, enhanced carrier injection into the semiconductor film through appropriate band alignment of sensitizer is achievable. Furthermore, several studies have shown that the cell efficiency can be enhanced by implementation of simple strategies such as using cascade structure of semiconductor and surface treatment to impair the recombination process.[26, 27]

High extinction coefficients and improved light absorption properties[31] is another advantage of semiconductor sensitizer that makes QDs promising sensitizer for NiO based device. It worth noting that due to poor mechanical properties of NiO and difficulty to fabricate the thick films, good light absorption properties of sensitizer is very essential for NiO based solar cell.[2]

Besides, by generating multiple electron-hole pairs per photon through the impact ionization effect in QD sensitized cells, the Shockley-Queisser limit can be exceeded. [32-34]

Despite the dye sensitizer that requires sophisticated chemical synthesis, making the semiconductor sensitizer is very simple and cheep. Several *in situ* and *ex situ* approaches have been reported to assemble the semiconductor sensitizer into the mesoporous film.[26, 27]

In situ methods include chemical bath deposition (CBD) and successive ionic-layer adsorption and reaction (SILAR). The main advantage of these methods is the high surface coverage of QDs on semiconductor film. Due to close contact between deposited QDs and mesoporous film charge injection from the QD into the wide-band gap material is very efficient.[27] In addition, forming a conformal coating of sensitizer on NiO film can act as a barrier layer, preventing injected holes in NiO film from recombining with the reduced redox species in the electrolyte.[27] However, in situ methods usually lead to a polydispersed deposition of sensitizer.[26]

In CBD method, semiconductor film is immersed into a mixture solution of cationic and anionic precursor and slow nucleation and growth of sensitizer on the surface leads to sensitizer deposition. In the SILAR method, semiconductor film is first immersed into a solution of cationic precursor followed by immersing into a solution of anionic precursor with washing in between to remove excess material. In this method, deposited QDs average size can be controlled by the number of deposition cycles.[26, 27]

Ex situ or colloidal QDs are pre-synthesized QDs which are bound to the surface of semiconductor film by molecular linkers. The main advantage of this method is that monodispersed QDs can be deposited on the film. However, two factors limit its application: first, it is reported that the molecular linker affects the charge separation and thus power conversion efficiency of the cell. [26, 27] Second, this method results in very poor surface coverage of QDs on the film and consequently lower power conversion efficiency is achieved compared with in situ methods.[26, 27]

The first report of NiO-SSC is published in 2011.[13] In this article, author used spray pyrolysis to synthesize thin film of NiO (~100 nm) which is further used as blocking layer to coat the FTO glass. Commercial NiO powder is then deposited on the blocking layer coated FTO and then film is sensitized by CdS through SILAR method. Sensitized film is then used to demonstrate the photocathode based SSC. The efficiency and IPCE of reported cell is low presumably due to the low quality of NiO film. Besides, due to the lack of application of NiO blocking layer, back current is generated in this cell structure which results in further decrease of photocathodic current.

Recently, *A. J. Frank et al.* have reported enhancement in IPCE and power conversion efficiency of NiO-SSC. They prepared NiO film by spin casting the NiO commercial powder. The film is then sensitized by CdS using CBD method.[14] In this work, good IPCE of 15% compared with 2% of first article is achieved. Furthermore, they claimed that the CdS-NiO solar cell resulted in two times faster hole transport compared with its DSC counterpart and almost 100% charge collection efficiency.

3- Formation of NiO-CdX (X=S, Se) photocathodes and Fabrication of P-NiO-SSC solar cells

Solar cells based on sensitization of *p*-type nickel oxide (NiO) have attracted significant interest in recent years.[1, 2, 16-18] Although the overall improvement is promising, the development of dye-sensitized nanocrystalline NiO solar cells still lags far behind that of TiO_2-based photoanodic cells.[8]

One approach that potentially could overcome existing problems is replacing the molecular sensitizers with semiconductor nanocrystals in *p*-type cells. As shown in Figure 3-1, upon illumination the semiconductor sensitizer (e.g. CdSe) absorbs light, which promotes electrons from the ground state to the excited state of the sensitizer. The holes left in the VB level of the semiconductor sensitizer will then inject into the VB of the NiO almost instantaneously. Meanwhile, electrons in the CB of the sensitizer are intercepted by acceptor species in the electrolyte resulting in efficient charge separation. Owing to quantum confinement effects, the band gap of semiconductor nanocrystals can be tuned by varying the particle size[29, 30] and thus favourable band alignment between sensitizer and the underlying wide band gap metal oxide could feasibly be achieved for enhanced carrier separation. In addition, the high extinction coefficient[31] of semiconductor nanocrystals makes efficient light absorption possible even with very thin electrodes.[35] Furthermore, by generating multiple electron-hole pairs per photon through impact ionization in semiconductor-sensitized cells, the Shockley-Queisser limit could in theory be exceeded.[32-34]

While intriguing, only very few studies of semiconductor-sensitized photocathodes have been reported thus far, and the factors dictating device operation are far from being unambiguously investigated.[13, 14, 36] In this regard, a comprehensive study was carried out in this paper,

where synthetic procedures used to produce CdSe-sensitized mesoporous NiO electrodes and

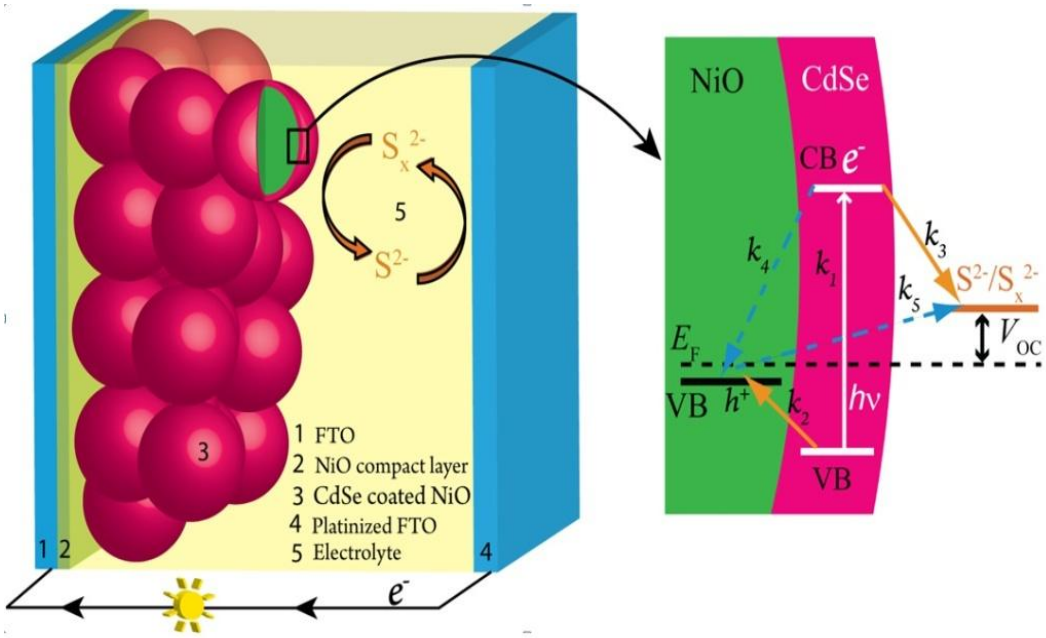

Figure 3-1- A schematic diagram illustrating the working principle of CdSe-sensitized mesoscopic p-NiO solar cells. The kinetic processes occurring at the NiO/CdSe/electrolyte interface are: k_1, excitation of CdSe upon illumination; k_2, hole injection from VB of CdSe into VB of NiO; k_3, sensitizer regeneration by acceptor species (Sx^{2-}) in the electrolyte; k_4, geminate recombination of holes in NiO with electrons in the CB of CdSe; k_5, recombination of holes in NiO with donor species (S^{2-}) in the electrolyte (dark current).

their morphological, structural, optical as well as electrical properties were systematically investigated.

3.1 NiO film synthesis and characterizations

3.1.1. NiO film synthesis

Several methods are attempted to synthesize the Nickel oxide film which are briefly reviewed in the first part. Among all proposed methods, Sol-Gel method reported *Suzuki et al.*[16] is chosen.

This method offers facile route to synthesis NiO in large quantity at room temperature. More importantly, morphology of the produced film is mesoporous which has high surface area.

To produce the NiO film, $NiCl_2$ nanoparticles (Sigma Aldrich), F108 triblock copolymer (Sigma Aldrich), DI water and Absolute ethanol were mixed (Sol) with the ratio of 1:1:3:6 respectively. This mixture is then aged for 3 days at room temperature to form Ni $(OH)_2$ (Gel). The polymer particles will be dissolved in between the nickel particles and upon sintering; oxidation of polymer particles form CO_2 which would be released from the film leaving the empty holes (pore) in the film structure. Thus mesoporous film will be produced.

After aging, the supernatant of the produced solution was separated and centrifuged at 6500 rpm for 2 min to separate the un-reacted precursors. To prepare the NiO film, centrifuged solution was heated to achieve a paste with desired viscosity which was then screen-printed onto the FTO glass. The FTO glass was washed with soap, DI water and ethanol prior to use. The printed films were then sintered in oven at 500 ^{o}C for 1 hour. It worth noting that the sintering process (sintering rate, duration and maximum temperature) has been optimized to achieve the highest solar cell performance. Printing process was repeated two times followed by sintering in between in order to make the desired film thickness. It is reported by *Lin Li et al.*[17] that stepwise printing and sintering the film increases the photo-generated current and IPCE. In their article, a film prepared and sintered in one step using two layers of scotch tape (to print the film by doc-blading method) is compared with another film prepared in two steps using one layer of scotch tape and sintering in between.

3.1.2. NiO film characterizations

Alpha-Step IQ surface profiler is used to measure the film thickness which was measured to be ~1.2 μm. This thickness is also confirmed by rough estimation of thickness from side-view FESEM image of the film.

The surface morphology of NiO film was characterized by field emission scanning electron microscopy (FESEM, Philips XL 30 FEG). Figure3- 2-a shows FESEM image of NiO surface. As can be observed the film exhibits a crack-free structure with average particle size of ~25 nm.

The morphology of NiO particles were determined by transmission electron microscopy (JEOL JEM 2010F). To prepare TEM samples, NiO film was scraped off from the FTO glass substrate. Particles were then dispersed in a drop of ethanol and sonicated to homogenize it followed by transferring one drop of the suspension onto a carbon-coated copper grid. TEM samples were used after several hours of drying in oven at 70 ^{o}C.

Figure 3-2-b shows TEM image of NiO nanoparticles. It can be observed that size distribution of particles is polydispersed in the range of 15-50 nm which is consistent with the FESEM measurement. High-resolution TEM image (Figure 3-2-c) shows crystalline structure of NiO nanoparticles with lattice spacing of 0.242 nm corresponding to the (111) single FCC phase (face-centered cube) (JCPDS, No-04-0835).[37]

To investigate the crystal structure of the sample, NiO film was characterized by x-ray diffraction (XRD) with a Bruker D8 using Cu KR1 radiation (λ = 0.154059 nm). The observed peaks are identical to the standard spectrum of the FCC NiO structure.[38]

In addition, XRD pattern also clearly reveals polycrystallinty of NiO nanoparticles in accordance with the TEM and FESEM measurements (Figure 3-2,3-3). X-ray diffraction (XRD) of NiO is illustrated in Figure 3-3.

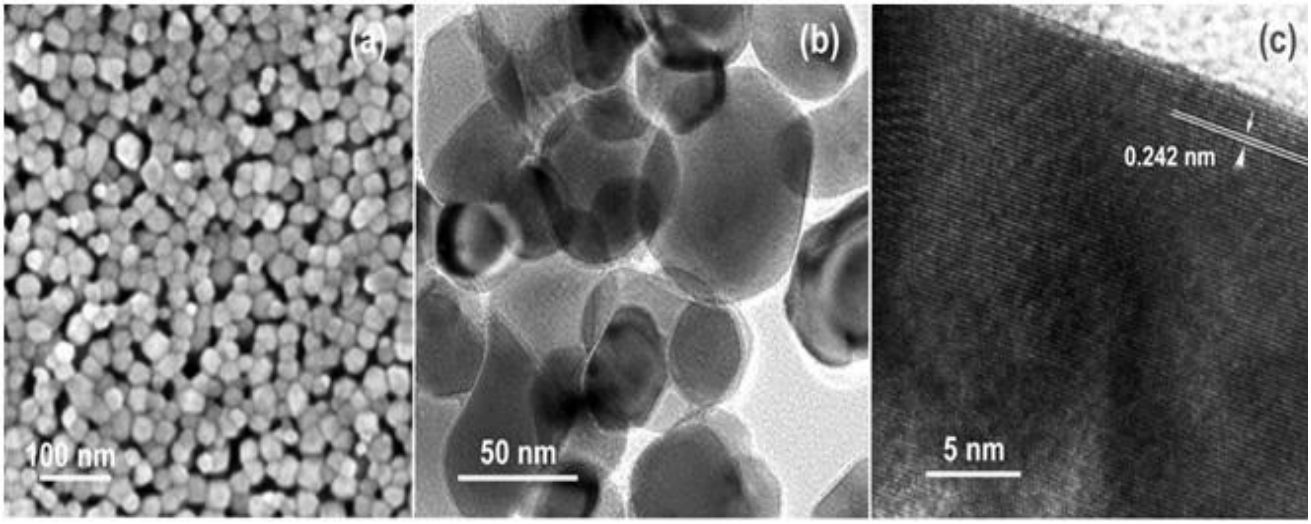

Figure 3-2-TEM image of NiO particles (a) and HREM image of NiO lattice structure (b) and mark the lattice fringes of as-prepared colloidal NiO particles (c)

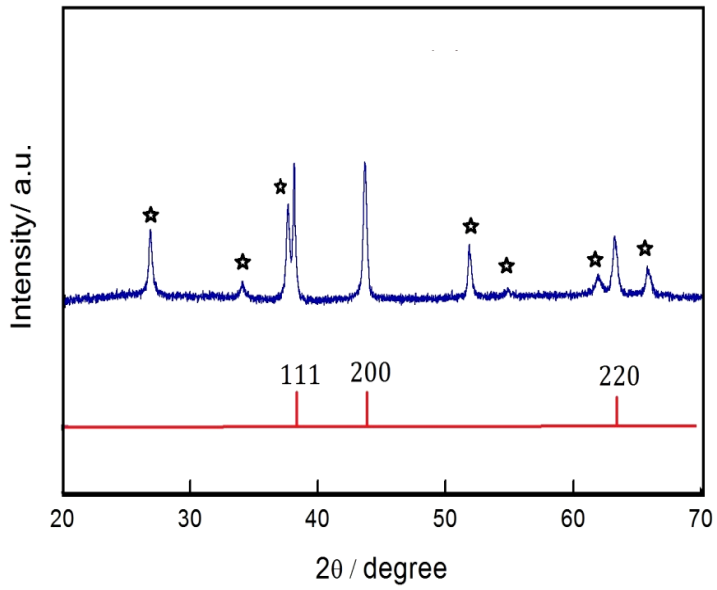

Figure 3-3-XRD peaks of NiO powder- Peaks resulted from FTO are indicated by star

3.2 Electrode Fabrication and characterization

To fabricate the NiO photocathode, NiO blocking layer[13] was deposited on FTO glass after successive washing of FTO glass with soap, DI water and ethanol, following the literature. In summary, 0.02 M solution of Nickel precursor (Ni $(acac)_2$ in ACN) was prepared. The FTO glass was heated and kept at 450 ^oC using the hotplate. Precursor was coated on FTO glass with sprayer (reagent Atomizer Kontes, TLC) connected to the vacuum pump by spraying repeatedly for 1 s followed by a 4 s pause totally for 40 min. Sample was then sintered at 450 ^oC for 30 min. The effect of blocking layer deposition will be discussed in the next part.

NiO film was printed on the blocking layer covered FTO as explained in NiO film preparation part. CdS, CdSe and cascade structure of CdS/CdSe have been used as a sensitizer materials. Here, SILAR method was used to assemble sensitizer into NiO film following the literature reports.[26]

To prepare CdS sensitized film, electrode was immersed in solution of 0.02 M cadmium nitrate tetrahydrate ($Cd(NO_3)_2.4H_2O$, Fluka, >99.0%) in methanol for 1 min to deposit Cd^{2+} . To remove excess Cd^{2+} electrode was rinsed in methanol for 1 min and dried for 1 min by N_2 stream. S^{2-} was then deposited by immersing the dried film into the solution of 0.02 M sodium sulfide nonahydrate ($Na_2S.9H_2O$, Sigma Aldrich) in 1:1, v/v mixture of methanol and DI water for 1 min. To remove excess S^{2-} , resulted film was then rinsed with methanol and dried for 1 min by N_2 stream. This procedure was repeated several times in order to achieve desired CdS deposition.[39]

CdSe deposition is done in glove box as selenium solution tends to oxidize in air. To make CdSe sensitized electrode, NiO film was first immersed in 0.03 M solution of cadmium nitrate tetrahydrate ($Cd(NO_3)_2.4H_2O$, Fluka, >99.0%) in ethanol for 1 min. Film was then rinsed with

ethanol for 1 min to remove excess Cd^{2+} and dried. To prepare the Se^{2-} solution, selenium dioxide (SeO_2, Sigma-Aldrich, 99.9%), sodium borohydride (NaBH4, Sigma Aldrich) and ethanol were mixed. Dried film was dipped in Se^{2-} solution for 1min followed by 1min rinsing with ethanol and drying. Deposition was repeated several times to achieve appropriate absorption of CdSe into the film.[40]

Similarly, to fabricate CdS/CdSe sensitized electrode, first CdS was deposited into the NiO electrode under the fume hood following the above mentioned procedure repeating for desired times.[39] CdS coated film was then transferred into the glove box. CdSe was deposited using the similar procedure mentioned. This step was also repeated several times to make electrodes with different sensitizer structure. Reverse cascade structure of CdSe/CdS was also attempted to study the effects on the solar cell performance.

In summary, for CdS coated NiO 5 and 10 deposition cycles were tried. For CdSe sensitized NiO electrodes 5, 7, 9, 10, 12 and 15 cycles were attempted. Likewise, for CdS/CdSe electrodes, 5/5 and 3/10 (CdS and CdSe respectively) cycles were deposited. In the case of reverse CdSe/CdS 5/5 cycles were examined.

The optimization of deposition cycles and deposition order (which layer to deposit first) was done based on the solar cell performance and will be discussed in the next part.

TEM and Optical measurements are applied to characterize the sensitizer coated NiO electrodes.

The morphology of CdS/NiO and CdSe/NiO were examined by transmission electron microscopy. Figures 3-4-a and 3-4-b show TEM images of CdS/ NiO nanoparticles after 10 SILAR cycles. As can be observed, CdS formed a conformal coating of ~3 nm thick layer on NiO. Likewise, Figures 3-4-c and 3-4-d show TEM images of CdS/ NiO nanoparticles after 10 SILAR cycles. Coating of CdSe on NiO is also conformal with the thickness of ~ 5 nm.

Optical densities of bare NiO as well as sensitized CdS-NiO, CdSe-NiO and cascade CdS/CdSe-NiO with respective 10, 10 and 5/5 deposition cycles were measured using a Shimadzu UV-vis-NIR spectro-photometer (Solidspec-3700). Figure 3-5 shows optical measurement results. It is evident that sensitizer incorporation enhanced the absorption intensity in the UV and visible regions. The absorption onset of CdS/NiO occurs at ~570 nm which is equivalent to the band gap of 2.17 eV.[41] Similarly, the absorption onset of CdSe/NiO occurs at ~720 nm slightly blue-shifted compared to the bulk CdSe, corresponding to the band gap of 1.7 eV.[42] Wider absorption spectrum of CdSe- covering most of the visible region -compared with CdS, resulted in wider absorption spectra of CdSe-NiO film than CdS coated electrode.

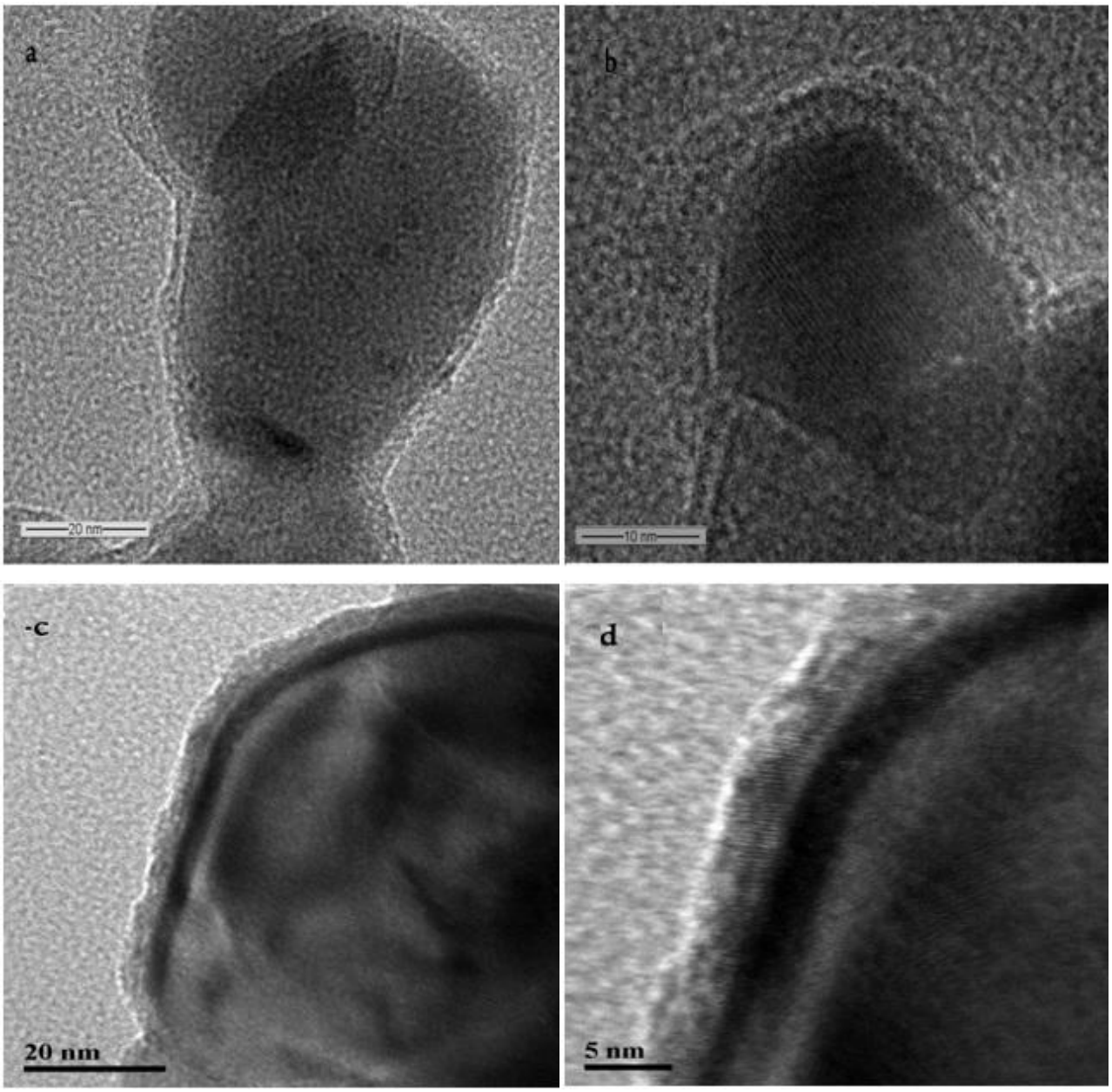

Figure 3-4-TEM images of CdS/NiO particles (a, b), and CdSe/NiO particles (c, d)

Furthermore, comparing different samples reveals that wavelength absorption characteristic of co-sensitized CdS/CdSe electrodes is much similar to CdSe coated NiO which points out that the main sensitization comes from CdSe than CdS.

Steady-state photoluminescence spectra of CdSe coated NiO were measured using spectrofluorophotometer (Shimadzu- RF5301) to study the charge injection from CdSe into the mesoporous NiO film upon illumination.

This measurement is also depicted in Figure 3-5. As a reference sample, photoluminescence response of CdSe coated Al_2O_3 was also measured and both films were excited at 450 nm. Al_2O_3 is a very wide band gap semiconductor (~9 eV) thus; charge injection from the excited state of CdSe to the conduction band of Al_2O_3 is not likely. Therefore, upon illumination electrons will be excited into the CdSe conduction band and as no charge transfer happens excited electrons recombine back with holes in the CdSe.

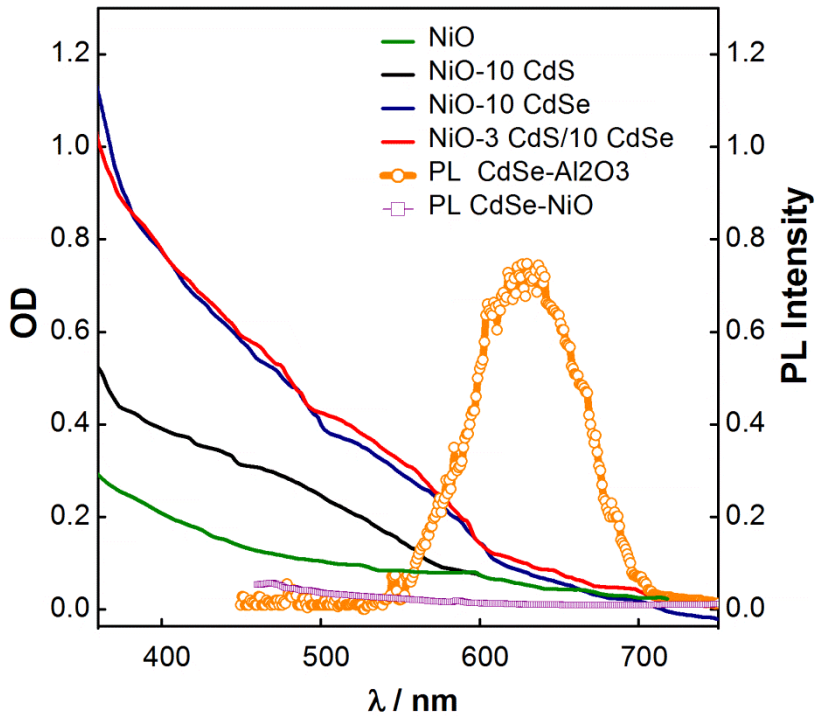

Figure 3-5-Optical measurements of bare and sensitized NiO electrodes, PL measurements of CdSe/NiO , CdSe/Al_2O_3

Consequently, CdSe/Al_2O_3 sample exhibits a sharp radiative peak at ~ 630 nm in the visible region. In contrast, no obvious emission peak can be observed from the CdSe sensitized NiO

electrode. This result indicates the quenching of the CdSe sensitized NiO electrode upon excitation. In other words, charge injection from CdSe into NiO mesoporous film is detected.

3.3 Cell Fabrication and characterization

To fabricate Semiconductor Sensitized NiO solar cell, counter and working electrodes were fabricated in a sandwich form with electrolyte injected in between similar to typical DSC. In order to make the counter electrode, which is Platinized FTO, the glass was washed with soap, DI water and ethanol successively and then cut into small pieces. Small hole was drilled into the FTO prior to the Pt coating to inject electrolyte. FTO pieces were then

heated up to 400 ^{o}C to remove remained contamination and then cooled down to room temperature. After that, the pt solution was coated on cooled glass and heated again at 400 ^{o}C for 15 min.

Polysulfide is a typical electrolyte used in n-type based SSCs. In our study this electrolyte is used without further modification for our NiO samples. The electrolyte is composed of 1 M S, 1 M $Na_2S.9H_2O$, and 0.1 M NaOH in DI water.[39]

To fabricate the solar cell, working electrode (semiconductor coated NiO) and counter electrode (Platinized FTO) were sealed in a sandwich form by means of thin layer of polymer film (Surlyn, DuPont). Vacuum pump is then used to fill the electrolyte into the inter-electrode space. The pre-made hole was sealed afterward using the thin layer of polymer film and microscope cover slip. To measure the current-voltage characteristics of solar cell Keithley Source Meter with a Newport solar simulator was used. All measurements were done under simulated AM 1.5 illuminations. Standard Si solar cell was used to calibrate the light intensity. All cells were covered by a mask to have similar illuminated active area of 0.1199 cm^2. Incident photon to current efficiency (IPCE) of cell was measured by a 300 W xenon lamp and a grating

monochromator (Newport/ Oriel). Standard silicon photodiode (Newport/Oriel) was used to calibrate the incident photon flux and photocurrent was measured using an auto-ranging current amplifier (Newport/Oriel).

Characterization results confirm that upon illumination, all sensitizers (CdS, CdSe and cascade CdS/CdSe) can inject hole into the valance band of p-type NiO. Illumination excites electron to the conduction band of sensitizer. Generated holes are injected into the valance band of p-type NiO. Generated electrons in sensitizer are captured by electrolyte and further transferred to the counter electrode and holes are collected from mesoporous NiO film which results in cathodic photocurrent.[13]

Effect of several parameters including thickness of NiO film, blocking layer, sensitizer type, deposition order and thickness on solar cell performance were examined by fabrication and characterization of cells.

3.3.1. Effect of sensitizer (CdS, CdSe, reverse cascade)

j-V characteristics of sensitized NiO with different deposition cycles of CdS (5, 10 SILAR cycles) and CdSe (7, 10, 15 SILAR cycles) are depicted in Figure 3-6-a, 3-6-b. It can be observed that the optimum layer deposition for both CdS and CdSe are 10 SILAR cycles deposition. Comparing the relative band edge position of NiO with both CdS and CdSe verifies that their valence band position is lower than that of NiO and thus hole injection is into NiO is anticipated. In devices that CdSe is used as a sensitizer, superior photovoltaic performances are exhibited compared to CdS sensitized devices. The better performance could be due to enhanced light absorption characteristics of CdSe coated electrodes.

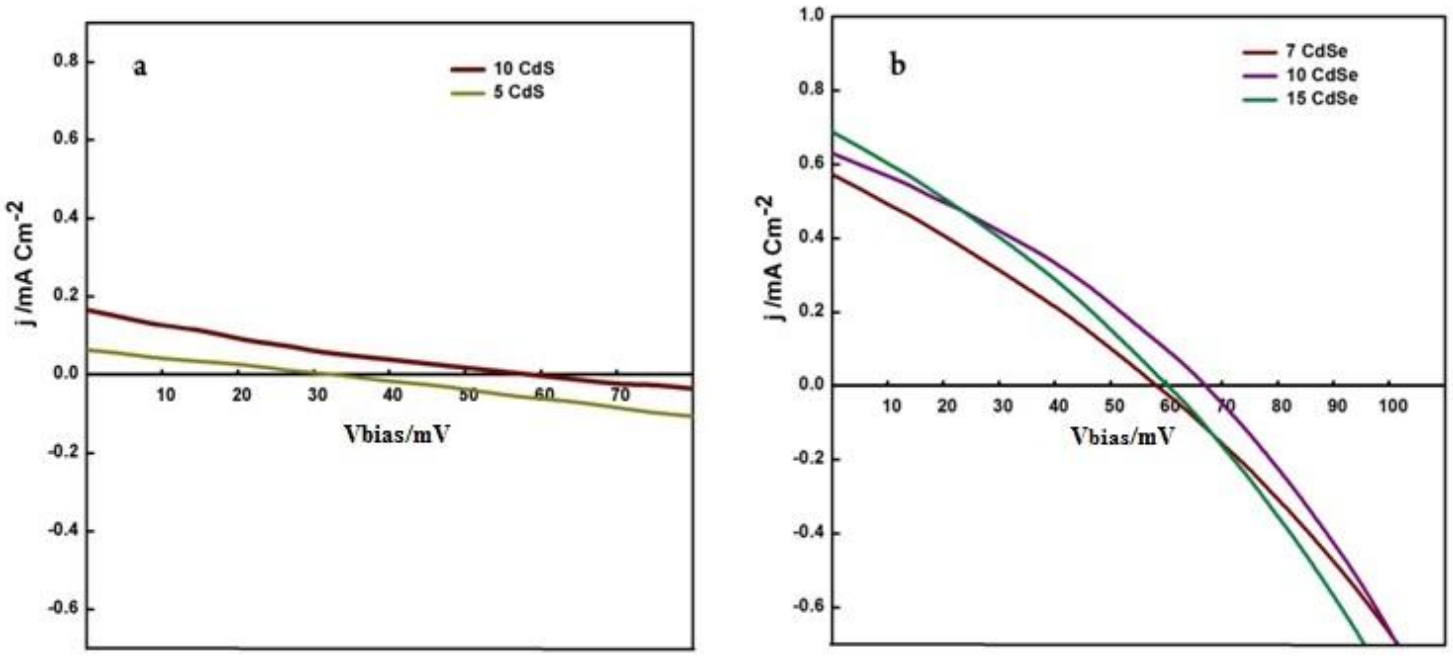

Figure 3-6--j-V characteristics of solar cells fabricated from different deposition cycles of CdS (a) and CdSe (b)

While the Voc of both CdS-NiO and CdSe-NiO cells were very close, higher jsc and FF of CdSe-NiO resulted in 8 fold higher efficiency.

Besides CdS and CdSe, Cascade structure of CdS/CdSe and reverse structure of CdSe/CdS were used as sensitizer. In CdS/CdSe-NiO device different deposition cycles of CdS and CdSe (3/5, 5/5, 3/10 cycles) was tried. The best performance has been achieved by 3CdS/10 CdSe SILAR cycles deposition. Figure 3-7 shows the j-V characteristics of CdS/CdSe sensitized NiO devices. Comparison with CdSe devices reveals that for cascade structures of 5/5, 3/10, 5/10 jsc was increased compared with CdSe-NiO device. The best device was obtained with 3/10 CdS/CdSe cascade sensitizer with $\eta = 0.02\%$. Details of solar cell parameters are presented in Table 1.

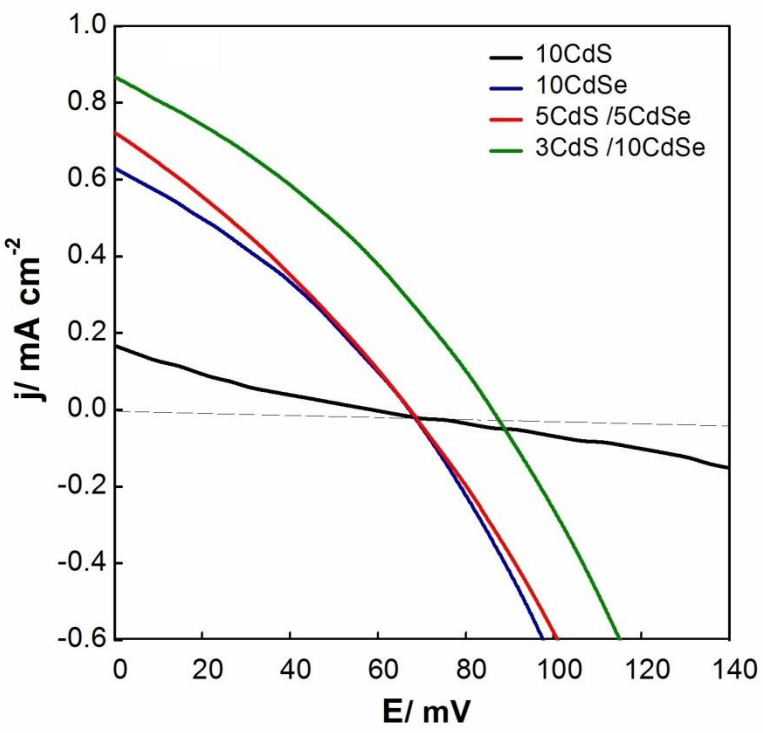

Figure 3-7-j-V characteristics of solar cells fabricated from CdS, CdSe and CdS/CdSe sensitized NiO cells. The thickness of the electrodes is ~1.2 mm.

Table 3-1 Photovoltaic parameters of CdS-NiO, CdSe-NiO and CdS/CdSe-NiO devices under simulated Am 1.5, 100 mW cm^{-2} illumination

CdS/CdSe	Voc (mV)	jsc (mA cm^{-2})	FF (%)	η (%)
10/0	58	0.16	20.8	0.0017
0/10	66	0.63	31.7	0.014
5/5	66	0.71	29.3	0.014
3/10	86	0.87	32.3	0.02

The IPCE spectra of SSCs are illustrated in Figure 3-8. It is obvious that the Photoresponse in CdSe-NiO and CdS/CdSe-NiO devices is enhanced extending to ~ 700 nm compared to ~530 nm

in CdS-NiO cells and also, the highest quantum efficiency is observed in co-sensitized devices. Peak IPCE of 30% is achieved at ~400 nm with 5CdS/5CdSe-NiO cell.

Comparing the 3Cds/10CdSe cell and 5 CdS/5CdSe shows that firstly, in 3Cds/10CdSe slightly lower IPCE pack is observed compared to 5 CdS/5CdSe due to less amount of CdS. And secondly, for 3Cds/10CdSe the IPCE response in long wavelength range is enhanced despite the almost identical optical spectra which could be the responsible for the better performance of the cell.

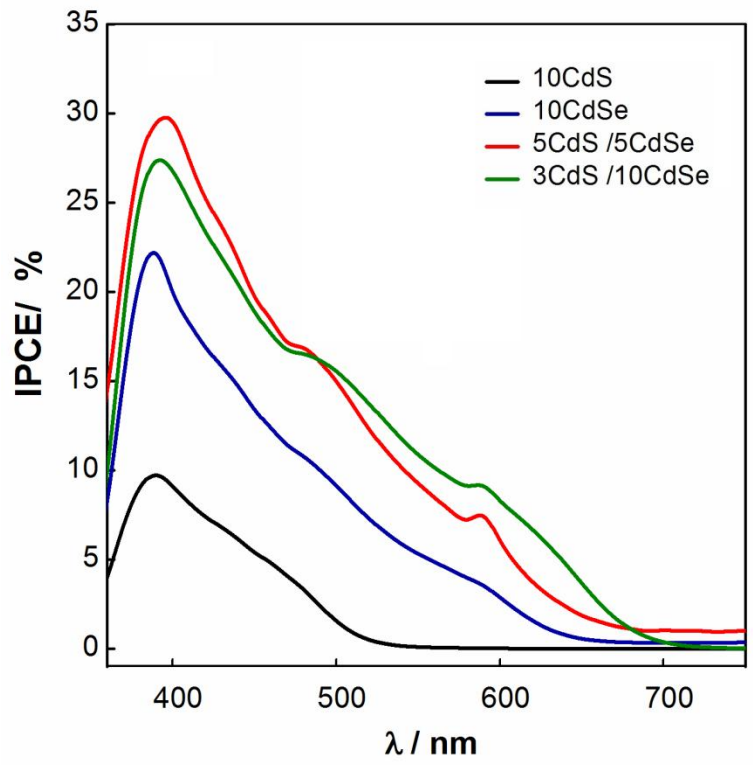

Figure 3-8-IPCE spectra of solar cells fabricated from different sensitizers including CdS, CdSe and CdS/CdSe

The maximum IPCE response for CdS, CdSe and CdS/CdSe cascade cells were 10%, 22% and 30% respectively. The observed IPCE of 30% is a very promising improvement and is the highest reported value for semiconductor sensitized p-type cell. Furthermore, looking at the co-

sensitized device despite the very identical optical spectra in the most of wavelength range to CdSe-NiO, both IPCE and photocurrent are enhanced.

These results imply that the presence of CdS is helpful to the photovoltaic performance. As mentioned, optical spectra of CdS/CdSe-NiO sample is much similar to CdSe-NiO samples meaning that the main sensitization comes from CdSe and contribution of CdS to photogeneration is minor. Two terminologies are used in published articles to explain this enhancement. Firstly, it is reported that presence of CdS under layer facilitates the growth and nucleation of CdSe[40] attributable to much similar lattice constant of CdS and CdSe than CdSe and substrate. Although this claim may be correct, our results confirm that this is not the reason behind the superior performance of co-sensitized device as by increasing the deposition cycles performance decline is observed (comparing the cell efficiencies for 10,12 and 15 SILAR cycles). This drop is most likely because by increasing the amount of sensitizer, although the light absorption may increase, blocking of pores with sensitizer as well as presence of some sensitizer without direct contact to semiconductor film result in efficiency decline. Secondly, for a TiO_2 SSC with cascade CdS/CdSe sensitizer it is suggested that upon deposition of sensitizer layers redistribution of band structure of CdS, CdSe and TiO_2 occurs and collection of excited electrons from CdSe to TiO_2 becomes more efficient.[43] However, our observation confirms that the band edge shift for cascade structure most likely is not occurring as for different semiconductor films including NiO, TiO_2 and SnO_2 with different band diagrams cascade structure resulted in higher photogeneration.

The most probable explanation for this enhancement is that the CdS layer deposited in between NiO film and CdSe acts as a buffer layer and passivates the NiO surface. Therefore, recombination of injected hole in NiO film with electron is reduced which results in higher

photocurrent and quantum efficiency. Based on the band diagram of CdS, CdSe and NiO it is possible that the CdS layer may hinder hole injection from CdSe into NiO. However, observed results confirm that the gain from surface passivation and thus decreased recombination is greater that the loss from impeded hole injection.

Thus, plausibly the surface passivation and hindered recombination is a cause of better performance in cascade structure.

It worth mentioning that this is still a hypothesis as the detailed band structure and performance of SSCs is not very well understood. Identifying the exact reason behind the jsc and IPCE enhancement requires more detailed investigations. One strategy is to measure the band edge position of NiO and sensitized NiO which is a part of the further plan of our project.

Besides, the reverse cascade structure of CdSe/CdS –NiO device was also fabricated. jsc and IPCE of this cell were lower compared with both CdS/CdSe-NiO and CdSe-NiO device. If we accept the CdS layer acts as a buffer layer this observation can be explained as follow: Presence of CdS after CdSe layer forms energy barriers for electron transfer from CdSe to the redox electrolyte. Thus, recombination between trapped electron in CdSe and injected hole in NiO would be accelerated and declined the cell performance. Comparison of CdSe/CdS-NiO device performance with CdS-NiO and CdS/CdSe-NiO is depicted in Figure 3-9.

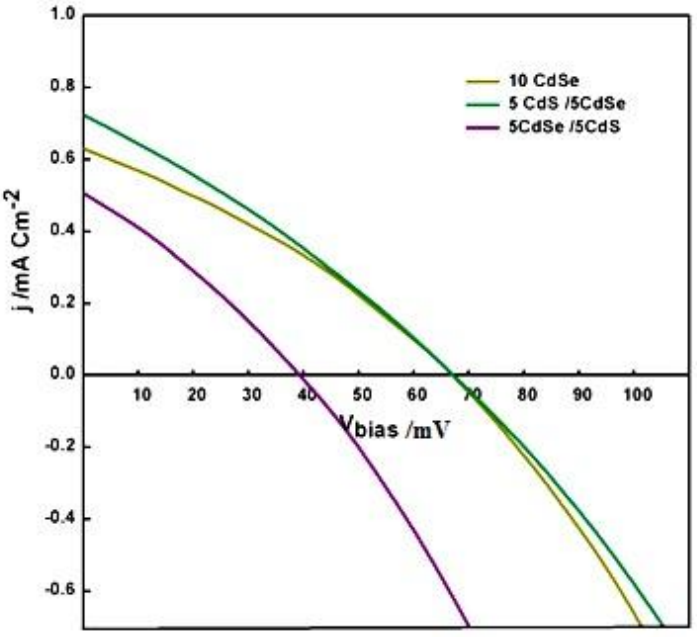

Figure 3-9-j-V characteristics of solar cell fabricated from CdSe-NiO, CdS/CdSe-NiO and reverse sensitizer structure (CdSe/CdS-NiO)

3.3.2. Effect of NiO film thickness

To study the effect of film thickness on cell performance, 3 different films with 1 printed NiO layer (~ 0.5 μm) ,2 NiO layers (~ 1.2 μm) and 3 layers of NiO (~ 1.8 μm) were prepared and CdSe sensitized devices were fabricated. The j-V responses of these cells are shown in Figure 3-10. As can be observed, increasing the film thickness from 0.5 μm to 1.2 μm improved the cell performance due to enhanced light absorption. (This is confirmed with optical spectra an measurement which is not shown.) However, furtherer increasing the thickness of NiO mesoporous film from 1.2 μm to 1.8 μm did not improve the cell performance since the increased light harvesting efficiency of thicker film is compensated by longer transport and lower charge collection. Same observation is reported by *Li et al.*[17] for similarly prepared NiO film for DSC.

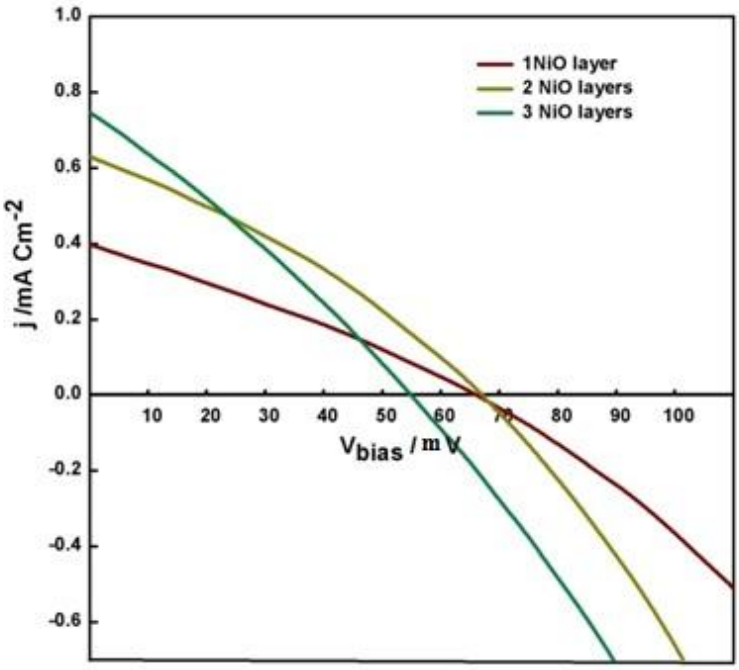

Figure 3-10-j-V characteristics of solar cell fabricated from photocathode with different thicknesses

3.3.3. Effect of blocking layer

It is reported that presence of hole blocking layer is essential for NiO based SSC. [13] In our project, two different batches of solar cells with and without blocking layer are fabricated to investigate the effect of blocking layer on the cell performance. The results show that the cells with no blocking layer exhibit ~3.5 fold lower photoconversion efficiency and lower IPCE spectra. This is because of the poor hole mobility in the NiO film and plausible electron transport through the sensitizer layer. The back transferred electron is further collected at the FTO substrate, while hole is transferred into the electrolyte. This process generates a reverse photocurrent which results in declining cell performance. Figure 3-11 presents the j-V and IPCE characteristics of these cells.

3.4 Effect of illumination intensities: comparison of IPCE predicted photoresponse with j-V measurements

To compare the photoresponse predicted by IPCE and j-V measurements, the short-circuit photocurrents (jsc) is calculated from the integration of IPCE spectra convolution over all wavelengths. For all SSCs, calculated jsc value from IPCE convolution is higher than measured jsc at simulated AM 1.5 and 1 Sun illumination. This difference can be explained by the different light intensities of IPCE and Solar Simulator devices. IPCE measurements were made using low intensity monochromatic illumination.

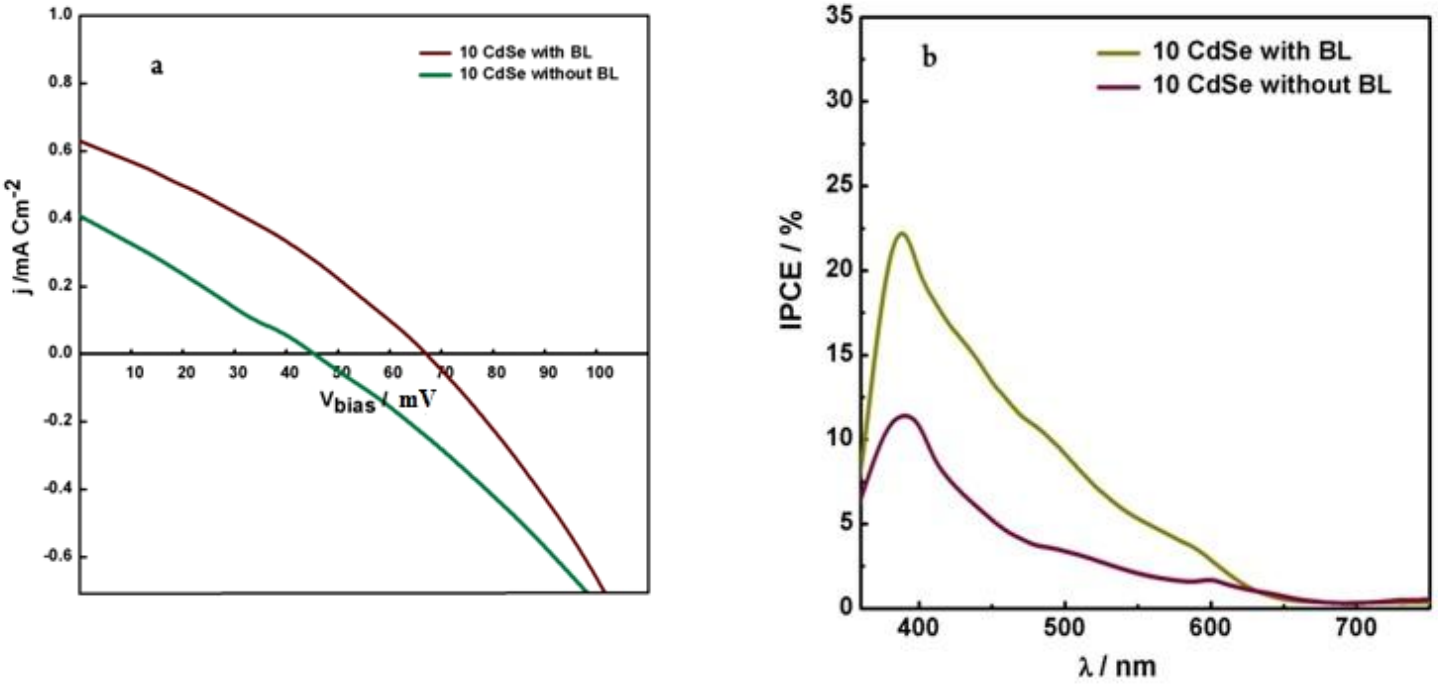

Figure 3-11-effect of blocking layer on solar cell performance, j-V characteristics (a), IPCE performance (b)

Therefore, higher jsc values calculated from IPCE spectra imply better photovoltaic performance of SSCs at low light intensities. To confirm this observation, current-voltage characteristics at

light intensity of 0.1 Sun was measured. As expected, for CdSe-NiO device 5 fold higher efficiency (0.07) and for CdS/CdSe- device 7 times higher efficiency (0.1) were obtained. Comparison photovoltaic parameters for different light intensities are summarized in Table 2.

Table 3-2 effect of light illuminations on solar cell efficiencies

Light intensity	*CdS/ CdSe cycles*	*Voc (mv)*	*Jsc (mA/cm^2)*	*Fill Factor*	*Efficiency (%)*
1 sun	0/10	66	0.63	31.7	0.014
0.1 sun	0/10	42	0.35	25.68	0.078
0.6 sun	0/10	60	0.55	29	0.019
1 sun	5/5	66	0.71	29.3	0.014
0.1 sun	5/5	42	0.47	24.6	0.107
0.1 sun	5/5	63	0.59	28	0.02

3.5 Study of Charge propagation in semiconductor-sensitized mesoscopic NiO solar cells

Impedance spectroscopy is commonly used to characterize the solar cell photophysical parameters. To characterize our cell we also performed impedance spectroscopic measurements experiments. However, due to the overlapping spectral features interpretation was difficult and

eventually we could not use this technique. One reason of this observation is very short diffusion length of charge carriers.

An alternative approach to investigate diffusion length and charge collection efficiency is to measure the spectral incident photon to current efficiency (IPCE) with once illuminating cells from working electrode direction (Front) and once from counter electrode direction (Rear). Then, the ratio of rear to front IPCE based on experimental data should be calculated. This data combined with optical measurements can be fitted to an expression based on the well-known "diffusion model"[44, 45] to calculate the diffusion length and charge injection efficiency.

Figure 3-12-a presents the measured rear and front IPCE spectra. As can be observed, a large difference between rear and front IPCE spectra is obvious. The first probable reason that comes into the mind is that the observed difference is because of the cell instability due to two time illumination during the measurement (once from one side and then other side). To check this inadequacy, several cells were fabricated and some were illuminated first from the front and then from the rear, while others were illuminated first from the rear side. Comparing all the measurements for rear side and front sides confirmed that the cells are stable and the variation was 6% at most which is reasonable.

The basic equations used in this part are:

$$\eta_{\mathrm{IPCE}}(\lambda) = \frac{i_{\mathrm{SC}}(\lambda)}{q\Phi(\lambda)} = \eta_{\mathrm{LH}}(\lambda)\,\eta_{\mathrm{INJ}}(\lambda)\,\eta_{\mathrm{COL}}(\lambda)$$

$$\eta_{\mathrm{APCE}}(\lambda,d) = \eta_{\mathrm{INJ}}(\lambda)\,\eta_{\mathrm{COL}}(\lambda,d)$$

According to the model used (standard diffusion model), the injection efficiency is independent of illumination directions or in other words, it is constant for rear/ front illumination: which is later confirmed by our calculations. Thus the ratio of rear to front APCE can be re-written as:

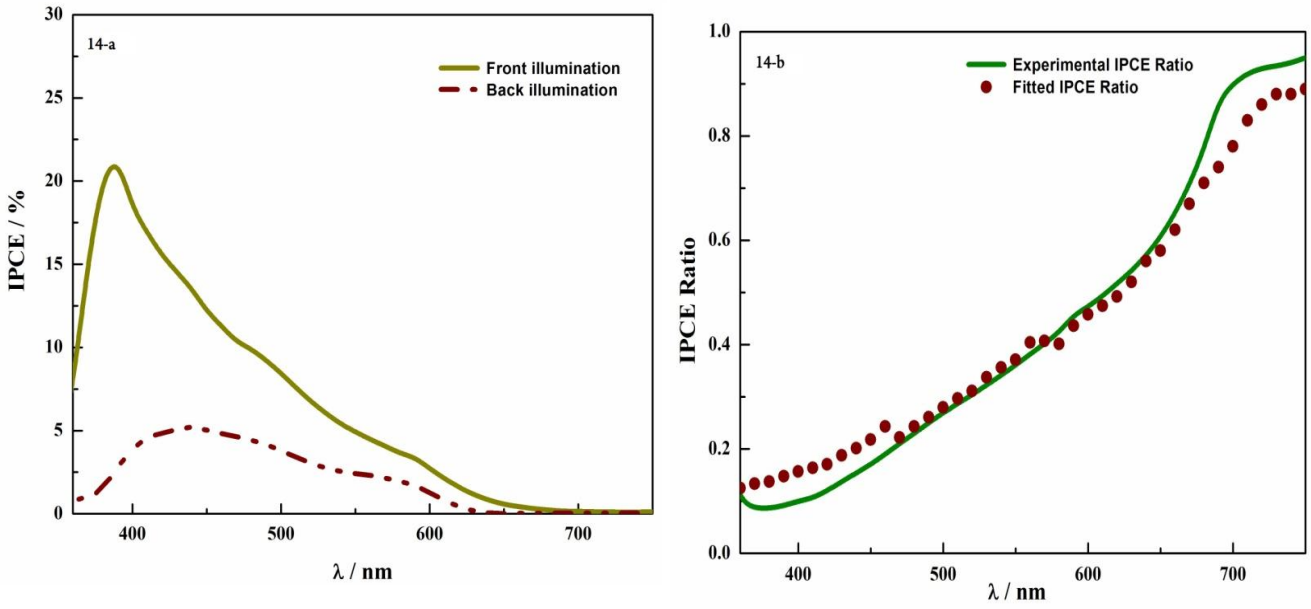

Figure 3-12-Back/Front IPCE spectra, Experimental IPCE performance (a), Back/Front IPCE ratio and fitting result (b)

$$\frac{\eta_{APCE,CE}(\lambda,d)}{\eta_{APCE,PE}(\lambda,d)}=\frac{\eta_{COL,CE}(\lambda,d)}{\eta_{COL,PE}(\lambda,d)}=\frac{\sinh(d/L)+L\alpha(\lambda)\cosh(d/L)-L\alpha(\lambda)\,e^{\alpha(\lambda)d}}{\sinh(d/L)-L\alpha(\lambda)\cosh(d/L)+L\alpha(\lambda)\,e^{-\alpha(\lambda)d}}\cdot e^{-\alpha(\lambda)d}$$

It is proven that:

$$\eta_{COL,CE}(\lambda,d)=\frac{[L\alpha(\lambda,d)\cosh(d/L)+\sinh(d/L)-L\alpha(\lambda,d)\,e^{\alpha(\lambda,d)d}]L\alpha(\lambda,d)\,e^{-\alpha(\lambda,d)d}}{(1-e^{-\alpha(\lambda,d)d})[1-L^2\alpha(\lambda,d)^2]\cosh(d/L)}$$

And

$$\eta_{COL,PE}(\lambda,d)=\frac{[-L\alpha(\lambda,d)\cosh(d/L)+\sinh(d/L)+L\alpha(\lambda,d)\,e^{-\alpha(\lambda,d)d}]L\alpha(\lambda,d)}{(1-e^{-\alpha(\lambda,d)d})[1-L^2\alpha(\lambda,d)^2]\cosh(d/L)}$$

Where:

L: diffusion length

D: film thickness

α : absorption coefficient (α= A/L)

Equations are obtained from reference No.[44].

The left hand side of above equation is known based on the experimental values. Thus by fitting the experimental value to the right hand side equation, where the only unknown is diffusion length (L) we can drive the value of diffusion length.

Figure 3-12-b presents the calculated rear to front IPCE ratio and the obtained fit. As can be observed, model deviates from the experimental values for wavelengths between 350 nm and 450 nm. The value of the hole diffusion length obtained was a few hundred nanometer ranging between 150 nm and 300 nm by trying different solvers to get the best possible fitting.

Using the equations mentioned above and estimated diffusion length, the collection efficiency for photoelectrode side and counter electrode side illumination were calculated. Also, the light harvesting efficiency for both illumination direction -which is only dependent on optical measurements- were calculated. Moreover, the IPCE is a product of light harvesting, charge collection and charge injection efficiencies. Therefore, by calculating the charge collection efficiency and light harvesting efficiency the charge injection efficiency can be calculated from the experimentally measured IPCE value.

Calculation shows that the front collection efficiency declined almost linearly from maximum value of 22% at wavelength of 350 nm to 10% at the wavelength of 750 nm. Likewise, the back collection efficiency was increased almost linearly from 1.6% at the wavelength of 350 nm to maximum value of 6.8% at wavelength of 750 nm.

For the calculated charge injection efficiency identical values were obtained independent of illumination direction, as expected. Interestingly, the calculated charge injection efficiency was strongly wavelength dependent while for DSC counterpart identical value for all wavelength ranges is reported. To verify the reproducibility of obtained results, several identical cells were tested that resulted in similar injection efficiency trend. The value of injection efficiency was ~ 20% at wavelength of 350 and increased to the peak of 100% at wavelength of ~ 400 nm and then gradually decreased to the value of 5% at the wavelength of 750 nm. It is noteworthy that

There are two probable explanations for this observation. Firstly, as mentioned the experimental IPCE could not be fitted adequately with applied model. Thus, the wavelength dependent injection efficiency may be result of model inadequacies. This is probable if the recombination dynamics are not linear in hole density as assumed in the present model.[46]

Secondly, if approximate validity of the model in the wavelength region where good fits could be obtained is accepted, there is a possible physical phenomena that may result is wavelength-dependent charge injection. As mentioned, sensitizer is assembled into NiO film by SILAR method which leads to a polydispersed size distribution of QDs[39] and distribution of band gap energies as well as HOMO and LUMO energies. Also, it is known that smaller QDs which have wider band gaps and bigger QDs that have narrower band gaps.[38, 47] Thus smaller QDs absorb only short wavelengths while bigger ones absorb both short and long wavelengths of light. Besides, the injection driving force for smaller QDs is higher than bigger QDs as the HOMO position for the smaller QDs is shifted downward (toward more positive potentials) resulting in a larger injection driving force. Consequently, the polydispersed QDs with different absorption spectra and injection driving forces may result in apparent wavelength-dependent injection efficiency.

4- Surface Engineering and Heterostructure Semiconductor Interface: Toward Better NiO-SSCs

Continuous efforts have been recently made to improve the device performance and more importantly to understand factors imposing the device performance and the loss mechanisms.[27] In this regard, several researchers attempted to investigate the conceptual differences between the semiconductor sensitizers and molecular dye sensitizers. [35, 48] Zaban *et al.* has recently reported that unlike molecular dye in conventional DSCs, a semiconductor sensitizer contributes directly to the recombination process.[48] Consequently, attenuation of this type of recombination would be of great importance for further performance multiplication. Mora Sero *et al.* have recently conducted a systematic review on several approaches paved the way into the SSCs efficiency improvement.[27, 49] They suggested that aforementioned recombination in SSCs is anticipated to be reduced by surface states passivation in semiconductor sensitizer as well as formation of a blocking layer between sensitizer and semiconductor film, generally stated as surface treatment or surface engineering.

As proposed by Hodes the major difference between DSCs and SSCs stems from the existence of surface states in the semiconductor sensitizers.[35] It is mentioned that these surface states exhibit an alternative recombination path by trapping photogenerated charges. Although these surface states have been extensively explored in the colloidal QDs,[27] their consequence on the SSCs is not well identified yet.

One approach which has been extensively employed in photoanode based SSCs to hinder the recombination attributed to the semiconductor sensitizer and ultimately to enhance the SSC performance is through the formation of heterojunction interface between wide band gap metal

oxide film, semiconductor sensitizer and the electrolyte.[26, 50] For instance, ZnS has been frequently deposited on TiO_2-SC surface and resulted in increased recombination resistance and enhanced IPCE.[50] In heterojunction semiconductors, relative position of electronic energy

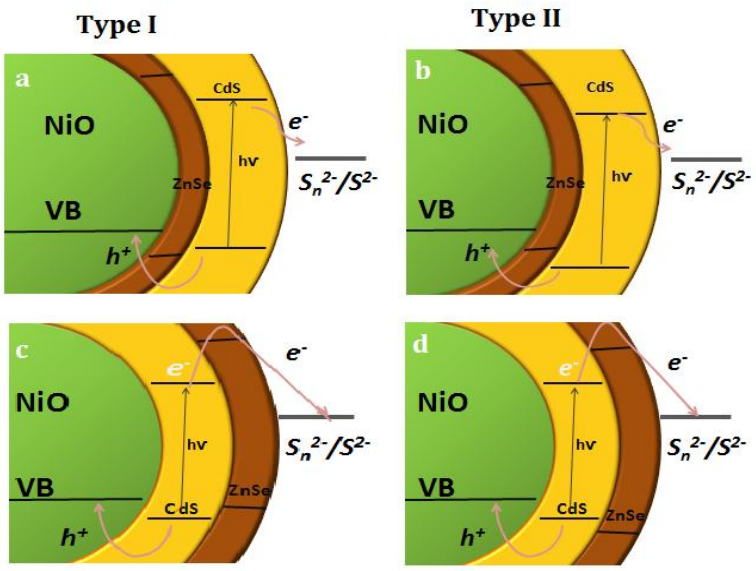

Figure 4-1-A schematic diagram illustrating the effect of ZnSe on CdS-NiO solar cell. Comparison of type-I (a) and type-II (b) heterojunction interfaces. In both configuration, ZnSe forms barrier for electron in CdS to recombine back with hole in NiO. Type-I impedes the hole injection into NiO as lower lying VB of ZnSe builds up an energy barrier for hole in VB of NiO. Such obstacle does not exist in type-II heterojunction interface. Reverse type-I(c) and reverse type-II(d) demonstrate barrier for electron-hole separation and thus accelerated recombination

levels and band gaps of two involved semiconductors layers determines the structure type (type-I or type-II). In the former (type-I), the material with smaller band gap is confined within a wider band gap semiconductor, while in the latter (type-II), valance band or conduction band of over-coated semiconductor is located within the band gap of underneath semiconductor layer. Figure 4-1 presents the schematic illustration of type-I and type-II heterojunction between ZnSe and CdS which are deposited on p-type NiO. As can be observed, type-II is more favourable as it does not obstruct the hole injection which happens in the type-I alignment.

While rigorous interfacial engineering methods have been effectively attempted for

photoanode based SSCs, to the best of our knowledge no studies on semiconductor-sensitized photocathodes have been reported thus far. In this regard, systematic study was carried out in this paper to investigate the effect of surface engineering and to enhance the performance of photocathode SSCs. The results suggest that the surface treatment is a powerful tool to hinder the recombination in photocathode SSC as well. Although significant performance enhancement has been observed for both photocathode and photoanode based SSCs, the exact passivation mechanism is yet under debate.[27]

In this study, ZnSe and ZnS was deposited on NiO prior to deposition of CdS and CdSe sensitizer respectively by applying a simple successive ionic-layer adsorption and reaction (SILAR). Optical absorption spectroscopy, transmission electron microscopy (TEM), j-V characteristics and incident photon-to-current efficiency (IPCE) measurements and open circuit photovoltage decay (OCP) were performed to characterize the sensitized electrodes and explore the effect of interfacial engineering on the cell performance. Cells employing ZnSe barrier layer in NiO sensitized with CdS exhibit an encouraging enhancement of external quantum efficiency being more than two fold higher than the cells without ZnSe layer. Likewise, better performance has been achieved in the CdSe-NiO SSCs when ZnS has been employed as barrier layer. However, in CdSe-NiO it seems that employment of CdS layer is more effectual than ZnS, more plausibly due to less lattice mismatch and improved interface properties.

4.1 Modified photocathode fabrication with ZnSe and ZnS

SILAR method was used to deposit sensitizer onto NiO film following the previously reported literature.[39, 51, 52] CdS and CdSe sensitized electrode fabrication is explained in the chapter 3. Same method has been applied herein to produce the electrodes with required properties.

To fabricated ZnSe treated electrodes, prior to CdS deposition, NiO film was first immersed in 0.1 M ethanolic solution of zinc acetate dihydrate ($Zn(CH_3COO)_2$ $2H_2O$, Sigma Aldrich, >99.5%) for 1 min followed by rinsing in ethanol and drying. The film was then immersed in Se^{2-} solution prepared by mixing selenium dioxide (SeO_2, Sigma-Aldrich, 99.9%), sodium borohydride (NaBH4, Sigma Aldrich) and ethanol following the literature. Subsequently, the film was rinsed in ethanol and dried.

To fabricated ZnS treated electrodes, prior to CdSe deposition, NiO film was first immersed 1min in 0.1 M aqueous solution of zinc acetate dihydrate and 1 min in 0.1 M aqueous solution of Na_2S . $9H_2O$, with 1 min of rinsing in DI water and drying between each immersion in a precursor solution.[43, 51]

4.2 Optical and morphological properties of photocathode

SILAR method is a widely used in situ method for deposition of semiconductor sensitizers onto mesoporous metal oxide films.[25, 43] Besides the simplicity, it provides high surface coverage and intimate contact between the deposited sensitizer and the metal oxide photoelectrode. However, direct contact between the wide band gap metal oxide and light absorbing semiconductor raise the recombination probability of the separated charge carriers .[27]

To control the recombination between the generated electron and hole in TiO_2-SSC surface engineering has been proposed as a powerful strategy in recent studies. [27, 53]

In this study two batches of photocathodes were fabricated: NiO coated with CdS or CdSe sensitizer and NiO coated with cascade structure of semiconductor sensitizer including ZnSe/CdS-NiO, ZnS/CdSe-NiO and CdS/CdSe-NiO. Cascade structure is constructed to

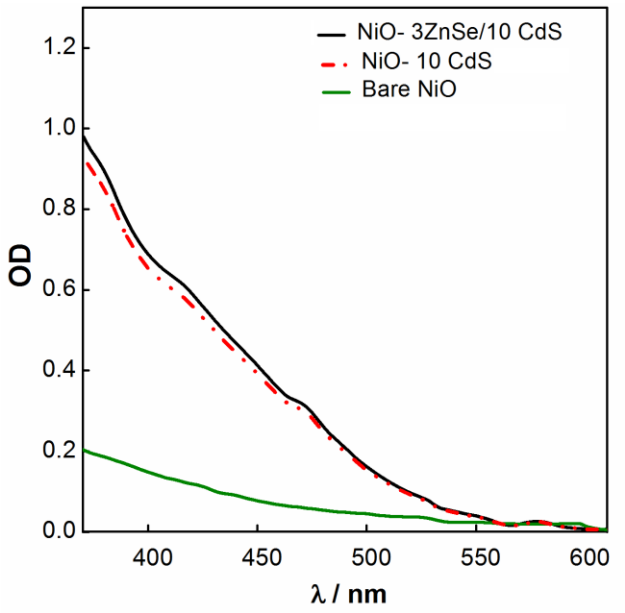

Figure 4-2- UV-Vis optical density spectra of pristine NiO, NiO Sensitized by 10 SILAR cycles of CdS (NiO-10CdS) and electrode treated by 3 SILAR cycles of ZnSe layer and sensitized by CdS (NiO-3ZnSe/10CdS).

investigate the effect of heterojunction interface on the photocathode and solar cell performance. Figure 4-2 shows the optical density spectra of CdS-NiO electrode as well as respective cascade electrode (ZnSe/CdS-NiO). The absorption onset of CdS-NiO sample characterized after 10 SILAR cycles is extended to 570 nm. The heterojunction structure - 3 SILAR cycles of ZnSe followed by 10 SILAR cycles of CdS – on NiO was also characterized and revealed an almost identical spectrum to that of 10CdS electrode. This indicates that in both structure, absorption is solely dominated by the CdS layer and ZnSe is not deemed to further enhance the light absorption. Thus, observed performance enhancement in presence of ZnSe layer (Section 3-3) could not be attributed to the enhanced light absorption properties of the cascade electrode.

The same phenomena is observed for CdSe sensitized and constructed cascade structure (Figure 4-3). That is, deposition of heterojunction structures did not alter the CdSe-NiO electrode optical

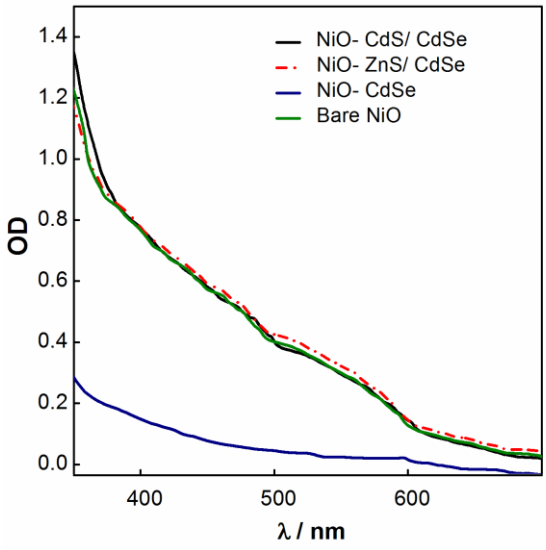

Figure 4-3- UV-Vis optical density spectra of pristine NiO, NiO Sensitized by 10 SILAR cycles of CdSe (NiO- CdSe) and electrode treated by 3 SILAR cycles of ZnS or CdS layer and sensitized by CdSe (NiO-ZnS/CdSe or NiO-CdS/CdSe)

properties and the CdSe is the only sensitizer layer which absorbs light and injects hole into NiO film.

From the optical density measurements (Figure 4-2, Figure 4-3) it is evident that no characteristic excitonic peak could be observed in the OD spectra of the sensitized electrodes regardless of the sensitizer type deposited indicating a dispersed size distribution of the deposited semiconductors.

It is plausible that the growth of semiconductor on different surfaces could be different . Thus, it is crucial to precisely compare the growth of sensitizer directly on NiO (NiO-CdS) with the cascade structure where sensitizer grows on another layer with much similar lattice mismatch

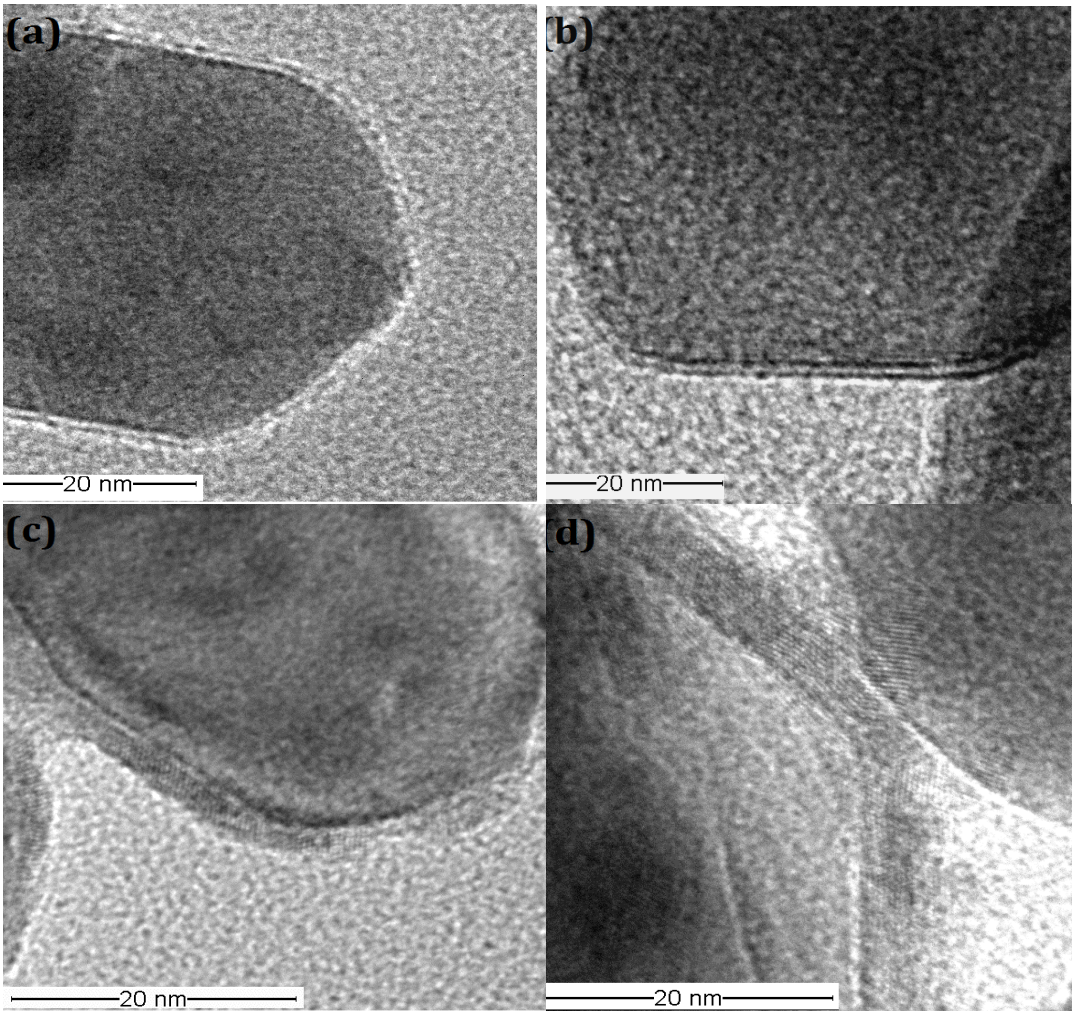

Figure 4-4- TEM images of (a) CdS-coated NiO nano-particles after 10 SILAR deposition cycles and (b) 3ZnSe SILAR cycles/10 CdS SILAR cycles coated NiO (3ZnSe/10CdS-NiO), (c) CdSe-coated NiO nano-particles after 10 SILAR deposition cycles and (d) 3ZnS SILAR cycles/10 CdSe SILAR cycles coated NiO (3ZnS/10CdSe-NiO)

(ZnSe/CdS-NiO where CdS grows on ZnSe). To evaluate the effect of heterojunction structure on sensitizer growth all electrodes were examined by high resolution transmission electron microscopy (TEM) and result is presented in Figure 4-4. TEM images of CdS-NiO and ZnSe/CdS-NiO electrodes indicate similar growth and thickness of CdS in both samples which specifies that ZnSe layer does not alter the growth of sensitizer (3(a), 3(b)). Similarly, the TEM images of ZnS/CdSe-NiO (3(c),3(d)) duplicate that of CdSe-NiO indicating the fact that the

sensitizer layer (CdSe) in both samples are similar.

It is worth mentioning that the above observation is very unique and it is usually expected that the existence of a semiconductor layer on metal oxide alters the growth of sensitizer as the surface properties changes. For instance, when ZnSe/CdSe-NiO electrodes were fabricated, the TEM images of ZnSe/CdSe-NiO electrodes illustrate thicker CdSe layer compared with CdSe-NiO electrodes (Figure 4-5). In accordance with the TEM measurements, optical spectra of these samples clearly shows the enhancement of light absorption by ZnSe layer deposition. (Figure 4-6). Thus observed performance enhancement in ZnSe/CdSe-NiO compared with CdSe-NiO could simply be attributed to the enhanced light absorption properties of the electrode (Figure 4-6).

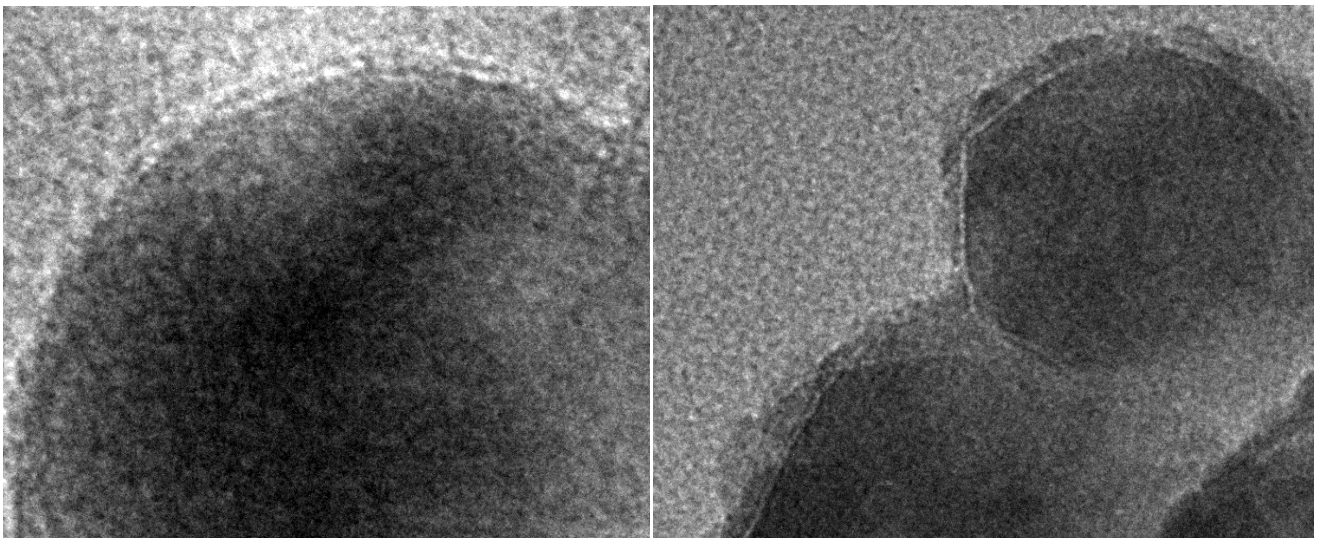

Figure 4-5- TEM images of (a) CdSe-coated NiO nano-particles after 5 SILAR deposition cycles and (b) 5 ZnSe SILAR cycles/5 CdSe SILAR cycles coated NiO (5ZnSe/5CdSe-NiO)

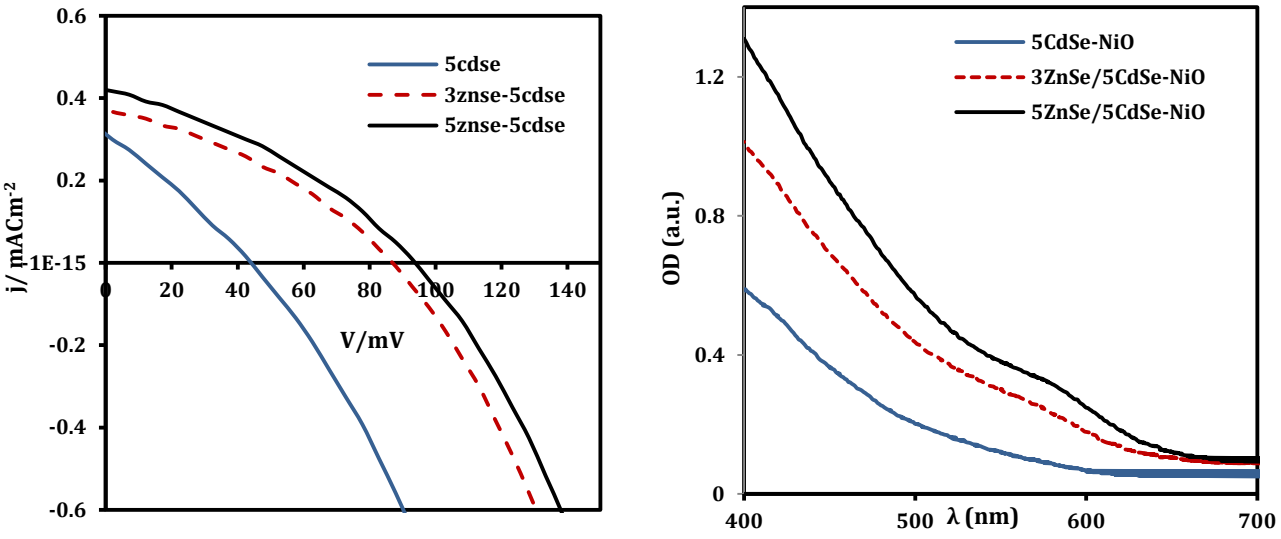

Figure 4-6- OD and cell performance of CdSe-NiO and ZnSe/CdSe-NiO

4.3 Photoelectrochemical characterization

To evaluate the photovoltaic performance, photoelectrochemical cells based on CdS and CdSe-sensitized mesoscopic NiO photocathodes were fabricated. For all samples NiO compact blocking layer was deposited on FTO glass prior to the NiO mesoporous layer deposition. Polysulfide electrolyte were used as the electron-transporting medium and considering the fact that Cu_2S based counter electrode is not stable in polysulfide electrolyte,[54] Platinized FTO was used as the counter electrode.

The photovoltage-photocurrent characteristics of NiO-SSCs were measured at 1 Sun illumination intensity and incident photon to current efficiency (IPCE) of NiO-SSCs were measured under DC mode at low light intensity (~ less than 0.1 Sun illumination intensity).

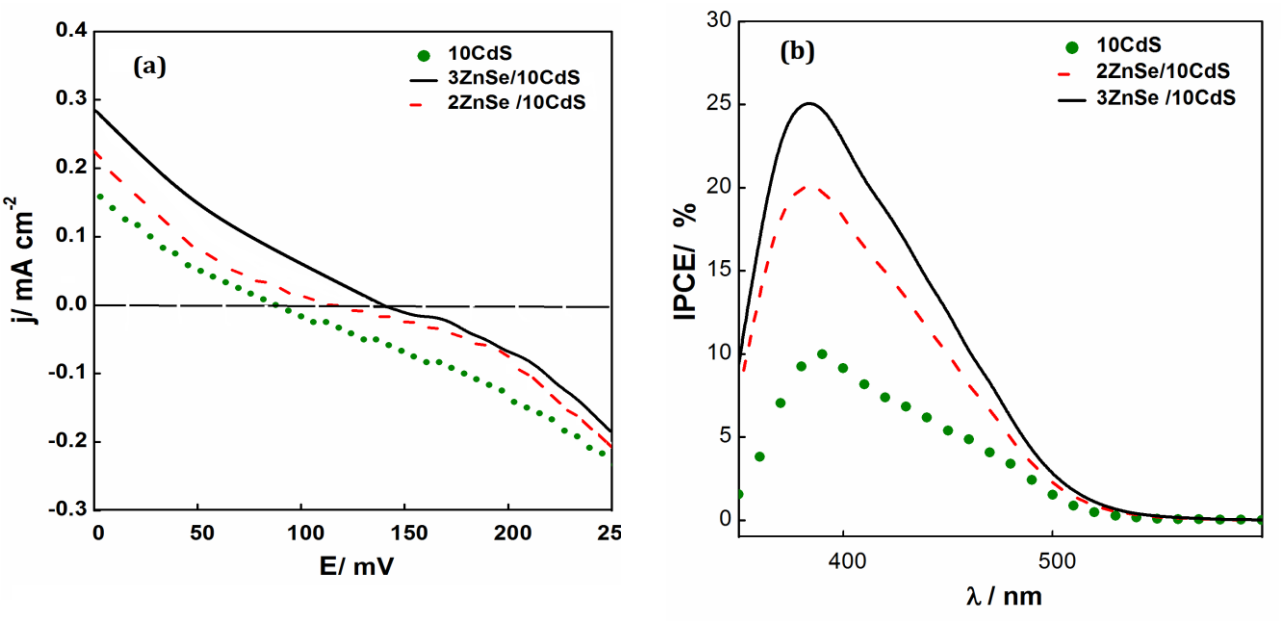

Figure 4-7- j-V characteristics and IPCE spectra of CdS sensitized and ZnSe treated CdS- sensitized NiO (ZnSe/CdS-NiO) cells. For ZnSe, 2 and 3 SILAR deposition cycles and for CdS, 10 SILAR deposition cycles were

It is worth mentioning that by changing the concentration of sulphur in the electrolyte the open circuit photovoltage of the cells are enhanced by ~ 80 mV compared to previously published results [25], although both electrolytes exhibit similar redox level.[48] Further research is required to clarify the effect of sulphur concentration on NiO solar cell performance, which is beyond the scope of this study.

Comparison of the UV-Vis and IPCE spectra reveals that IPCE spectra of all SSCs almost matches their respective optical density spectra indicating that the generated photocurrent in the SSCs originates from the light absorption of sensitizers deposited on mesoporous NiO. In addition, due to the strong absorption of photons with short wavelength compared with long wavelength photons and also short hole diffusion length, the IPCE spectrum appears sharp in the short wavelength region unlike broad IPCE spectra observed for CdS or CdSe sensitized TiO_2 SSC. [25]

To describe the effect of surface treatment on the TiO_2-SSC performance, Mora Sero *et al.* have

reported a physical model from the analysis of capacitance-voltage curves obtained from impedance spectroscopic measurements, considering the effect of surface states.[49, 55] Likewise, impedance spectroscopy measurements were attempted for NiO-SSCs which suffered from severely overlapping spectral features that made interpretation of the spectra very difficult.

4.4 ZnSe/CdS-NiO solar cell: Performance enhancement by heterojunction interface formation

The photovoltage-photocurrent characteristics of CdS-NiO SSCs and ZnSe treated CdS-NiO SSCs (denoted as ZnSe/CdS-NiO) are depicted in Figure 4-7. It can be figured out from Figure 4-2 and Figure 4-7(a) that the presence of ZnSe enhanced the photovoltage-photocurrent characteristic of CdS-NiO solar cell without altering the OD of electrode. The same trend can be observed for the IPCE spectra of CdS-NiO and ZnSe/CdS-NiO SSCs as shown in Figure 4-7-b. The IPCE spectra of ZnSe/CdS-NiO cells enhanced more than twofold compared with CdS-NiO cells despite the identical light absorption and IPCE spectra onset.

The fact that ZnSe does not change the light absorption properties of CdS-NiO electrodes (as shown in Figure 4-2) suggests that the presence of ZnSe is beneficial to reduce the recombination or to enhance the charge separation and charge collection, or both.

ZnSe/CdS is one of the most frequently studied heterojunction semiconductor structure.[56]The synthesis of the type-II ZnSe /CdS system has been extensively reported[57] and it is plausible that ZnSe/CdS has formed type-II junction. However, the exact interface alignment of ZnSe/CdS deposited on NiO and used as electrode in this study is not very well-known in device conditions. This is because common methods that are usually used to characterize the interface properties including Ultraviolet photon spectroscopy (UPS) and Photoluminescence spectra (PL)

are not applicable in here.[57]

Formation of type-II structure results in blue-shift of PL spectra due to confinement of electron and hole in different parts and formation of narrow quantum well near the interface.[31,32] However, due to charge injection from both CdS and ZnSe/CdS into NiO film, PL spectra is completely quenched and comparison of PL spectra is not feasible approach to examine the difference between two structure deposited on NiO.

Likewise, employment of Ultraviolet photon spectroscopy (UPS) which has been used to investigate the interface band alignment in the dry film[58] may not result in accurate determination of interface band structure when the sensitizer used in device .This is because in heterojunction sensitizer such as ZnSe/CdS, [56] size dependent band edge and the plausible band edge shift of oxide semiconductor in aqueous electrolyte[59] further complicates the system. As a result, the band alignment of dry film may alter when in contact with the electrolyte (device condition).

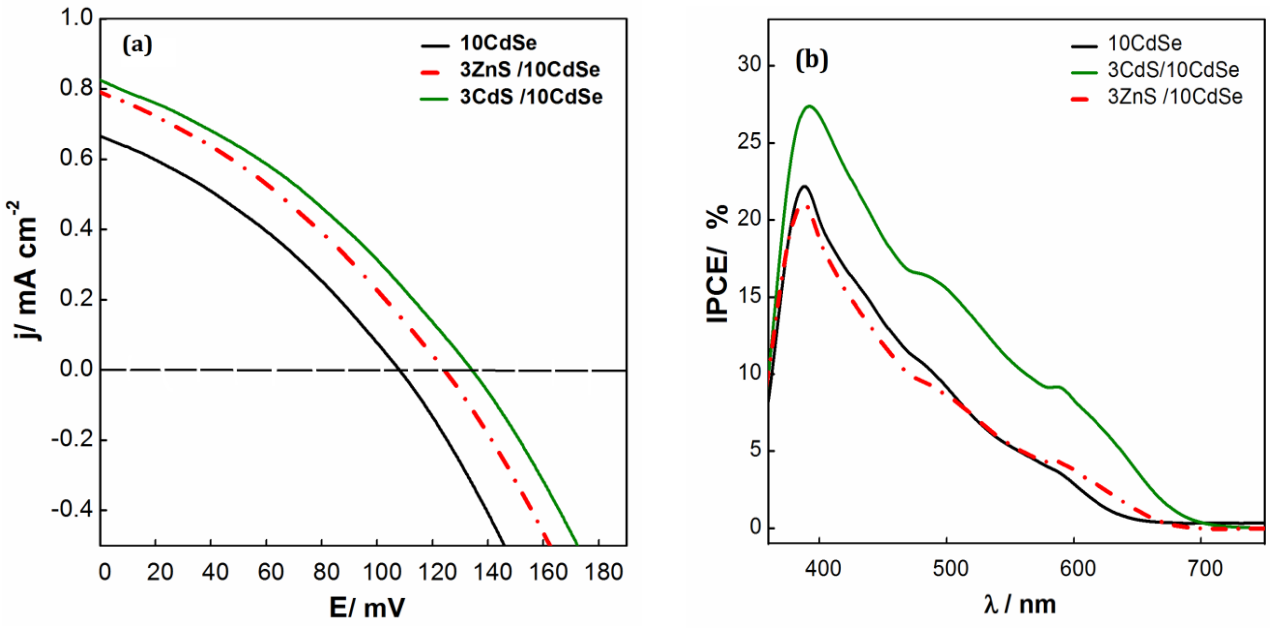

Figure 4-8- j-V characteristics and IPCE spectra of CdSe sensitized and ZnS, CdS treated CdSe- sensitized NiO (ZnS/CdSe- NiO, CdS/CdSe-NiO) cells.

Moreover, if the heterojunction interface results in strain and the formation of defect states, photogenerated charge carriers recombines at the interface. Thus, heterojunction structure increases the recombination rather than decrease.[56]

As a result, it can be most plausibly inferred that the ZnSe layer passivates the CdS-NiO interface, by formation of either type-I or type-II interface. Type-II is more likely based on the band alignment of two sensitizer in colloidal QDs. This passivation layer creates energy barrier that hinders the recombination between injected holes in NiO and electrons in CdS and electrolyte. Lower performance of reverse CdS/ZnSe-NiO SSC compared with both CdS-NiO and ZnSe/CdS-NiO SSCs further substantiates the role of ZnSe as a barrier layer (Figure 4-9). It is worth mentioning that a systematic study coupled with simulation of interfaces under device conditions is essential to explicitly determine the detailed band structure.

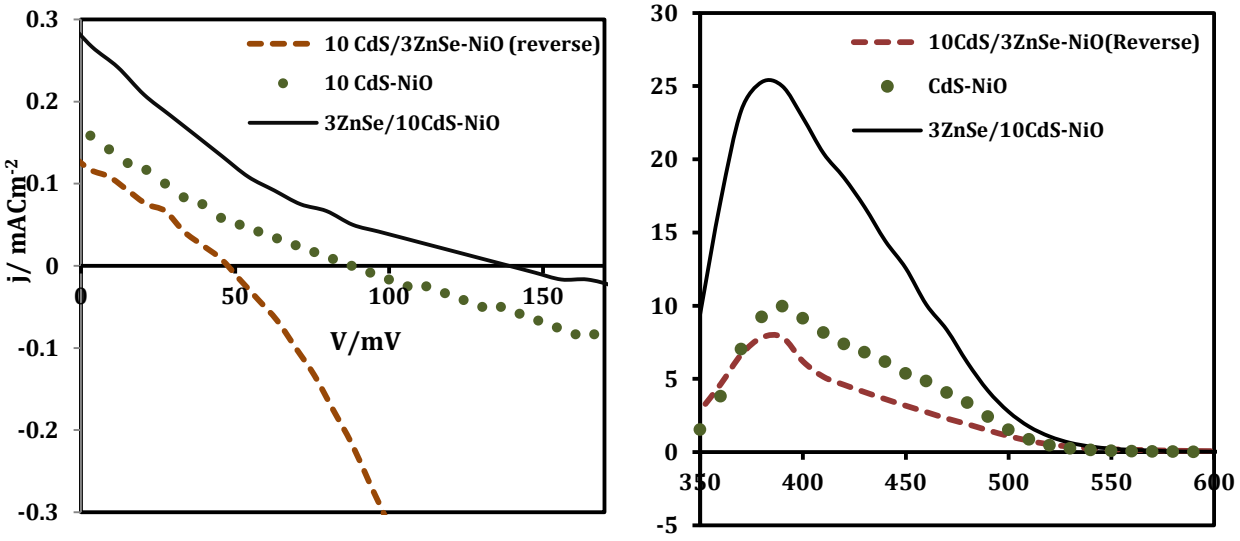

Figure 4-9- Comparison of cell performance of ZnSe/CdS -NiO, CdS-NiO and CdS/ ZnSe-NiO (reverse structure)

4.5 Effect of heterojunction interface: comparison of CdS/CdSe-NiO and ZnS/CdSe-NiO solar cells

The photovoltage-photocurrent characteristics of CdSe- sensitized and associated cascade electrodes denoted as ZnS/CdSe-NiO and CdS/CdSe-NiO are depicted in Figure 4-8.

Similar to ZnSe, it is evident that ZnS and CdS treatment has greatly enhanced both photocurrent and photovoltage generation and thus the solar cell performance without contributing to the light absorption as stated by the obtained results.

As mentioned, exploring the detailed heterojunction band structure in the device condition is complicated and not very well identified yet. The role of CdS in CdS/CdSe-sensitized NiO solar cells has been recently investigated and it is suggested that CdS/CdSe aligned more plausibly as type-I, thus forms a recombination barrier layer.[25] Same rationalization could be credible for the role of ZnS layer. That is, ZnS barrier layer hinders the recombination and hence, enhances the solar cell performance.

It is interesting to note that the enhancement achieved by CdS/CdSe structure is more pronounced than ZnS/CdSe structure. One plausible reason for the better performance of the CdS/CdSe-NiO SSC compared with the ZnS/CdSe-NiO SSC is the better interface properties in CdS/CdSe structure arising from the lower lattice mismatch between CdSe and CdS than CdSe and ZnS.[60] Moreover, formation of type-I may impede the charge injection from the sensitizer into the NiO valance band (Figure 4-11) which is unfavourable for the device. This effect is more severe in ZnS/CdSe electrode than CdS/CdSe electrode because of wider band gap of ZnS which forms larger barrier.[61, 62]

Similar to ZnSe/CdS-NiO SSC, lower performance of reverse CdSe/ZnS-NiO SSC (as well as CdSe/CdS-NiO) compared with both CdSe-NiO and ZnS/CdSe-NiO SSCs further demonstrates

the role of ZnS as a barrier layer (Figure 4-10).

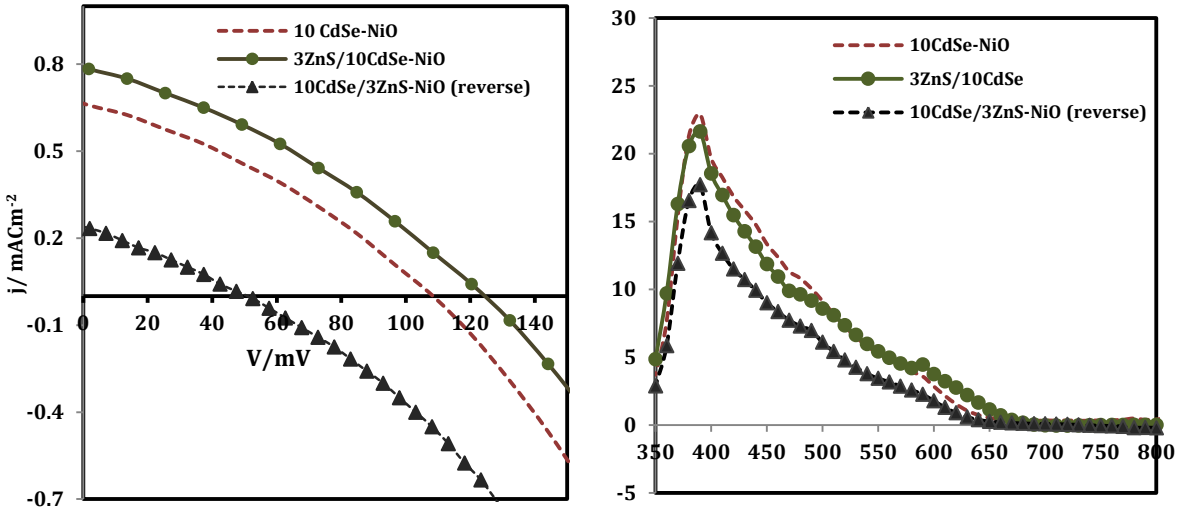

Figure 4-10- Comparison of cell performance of ZnS/CdSe -NiO, CdS-NiO and CdS/ ZnSe-NiO (reverse structure)

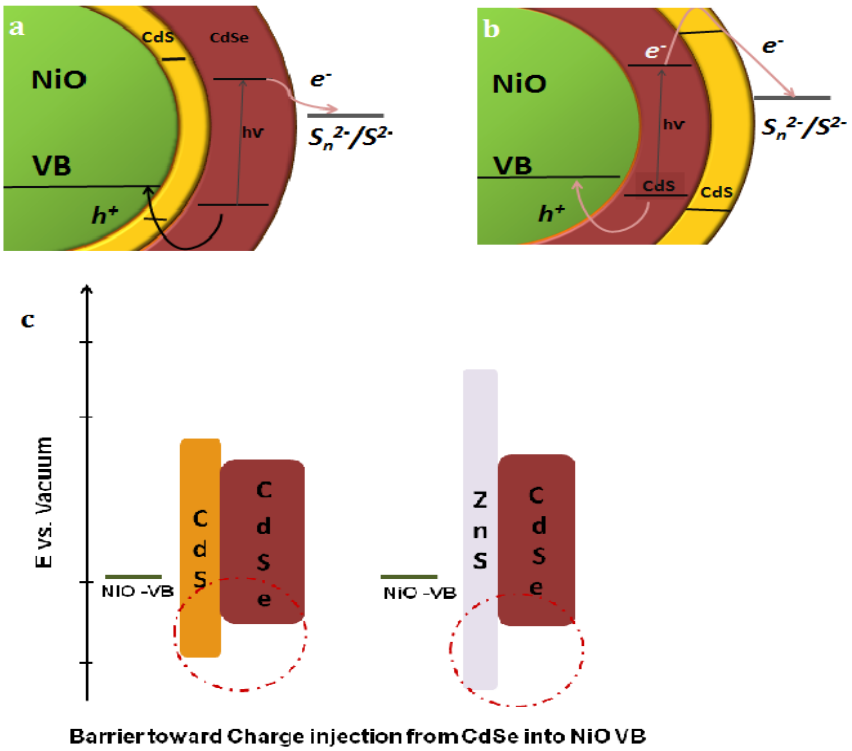

Figure 4-11- A schematic diagram illustrating (a) the formation of type-I interface between CdS and CdSe. (b) Interface between CdSe/CdS (reversed ordered deposited compared to (a)). (c) Comparison of ZnS and CdS as a barrier layer, investigating the effect of barrier height on the hole injection and solar cell performance .

To further evaluate the p-NiO SSC, OCP decay was also conducted and hole life time was calculated (Figure 4-12). The light intensity used was sufficient to produce a Voc approximately equal to that obtained under AM 1.5 1 Sun illumination and the light was illuminated long enough on the sample to reach a steady voltage. Then, LED was turned off and the OCP decay was recorded versus time in the dark. During OCP decay measurement, solar cell was maintained at the open circuit condition and the internal gradient of charge carriers was very low. Thus, recorded Voc vs. time is a measurement of series of steady state points. Finally, the hole life time was calculate from OCP decay following the equation reported by Zaban *et al.*[63] It is apparent that Voc decay is very fast and the hole life time is in the order of hundreds of millisecond. This result indicates that further recombination control is substantial to achieve desirable photocathode based SSC.[55]

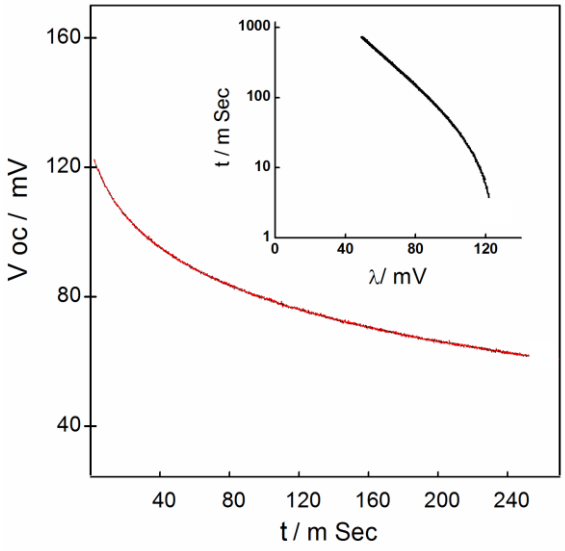

Figure 4-12- Experimental results of open circuit photovoltage decay for 10 CdSe and 3CdS/10CdSe NiO SSC. The inset shows the hole life time calculated from OCP decay.

5- Conclusion and Future work

In this study, crack free mesoporous nickel oxide film was synthesized through polymer modified sol-gel method. To construct a p-type based sensitized solar cell, semiconductor-sensitized NiO solar cells were fabricated by conformally coating CdS, CdSe and cascade CdS/CdSe sensitizers onto mesoporous NiO films by the SILAR method. With polysulfide as electron acceptor, for the first time NiO-based photocathodic SSCs were unambiguously demonstrated. Improved performance was achieved with cascade CdS/CdSe cells, indicating the CdS layer deposited in between NiO and CdSe effectively suppresses the recombination and enhances the cell performance as compared to CdSe cells. While encouraging, these *p*-NiO based SSCs still suffer from low power conversion efficiency. It is revealed from front and rear IPCE measurements that the cells are constrained by inefficient charge collection as a result of a short hole diffusion length in the mesoscopic NiO film. This partly arises from the fast recombination of injected holes in NiO with electrons residing in CdSe and the electrolyte, as supported by the low V_{oc} of the cells, as well as the fact that the cascade CdS/CdSe resulted in enhanced photocurrent and photovoltage.

To enhance the solar cell performance, the effect of interface engineering on the cell performance was systematically investigated. Noticeable enhancement of j_{sc}, Voc and IPCE has been achieved by depositing a few nanometer thick ZnSe layer between NiO film and CdS sensitizer. Considering the fact that presence of ZnSe does not alter the light absorption properties of the electrode as illustrated by the optical density measurements, the enhancement could be most plausibly because ZnSe builds up a blocking layer between the CdS sensitizer and NiO film and retards a recombination process. Colloidal ZnSe/CdS quantum dots are reported to form the type-II band alignment, and it is likely that the structure at the interface of ZnSe/CdS

layers could be type-II under device conditions. However, type-I structure is also plausible. Comparison of the performance of ZnS and CdS treated NiO-CdSe cells implies that the performance enhancement achieved by formation of heterojunction interface is greatly affected by the interface properties.

Although the accomplishment of the surface treatment is encouraging, the photo conversion efficiency of the cells are still low which stems from the fast recombination and low hole diffusion length. Insightful fundamental studies is essential to define the loss mechanisms and rigorous surface engineering is requisite to further enhance the cell performance. To improve cell performance, judicious interfacial engineering is desired in future studies to mitigate recombination and to further promote photovoltage and photocurrent. Furthermore, employment of efficient redox electrolyte instead of polysulfide and optimization of NiO film could result in enhanced performance of p-SSC as its molecular dye sensitized counterpart.

6- References

[1] J. He, H. Lindström, A. Hagfeldt, and S.-E. Lindquist, "Dye-Sensitized Nanostructured p-Type Nickel Oxide Film as a Photocathode for a Solar Cell," *The Journal of Physical Chemistry B,* 103, 8940-8943, 1999.

[2] F. Odobel, L. c. Le Pleux, Y. Pellegrin, and E. Blart, "New Photovoltaic Devices Based on the Sensitization of p-type Semiconductors: Challenges and Opportunities," *Accounts of Chemical Research,* 43, 1063-1071, 2010.

[3] A. Morandeira, J. Fortage, T. Edvinsson, L. Le Pleux, E. Blart, G. Boschloo, A. Hagfeldt, L. Hammarstrom, and F. Odobel, "Improved Photon-to-Current Conversion Efficiency with a Nanoporous p-Type NiO Electrode by the Use of a Sensitizer-Acceptor Dyad," *The Journal of Physical Chemistry C,* 112, 1721-1728, 2008.

[4] H. Yang, G. H. Guai, C. Guo, Q. Song, S. P. Jiang, Y. Wang, W. Zhang, and C. M. Li, "NiO/Graphene Composite for Enhanced Charge Separation and Collection in p-Type Dye Sensitized Solar Cell," *The Journal of Physical Chemistry C,* 115, 12209-12215, 2011.

[5] S. Uehara, S. Sumikura, E. Suzuki, and S. Mori, "Retardation of electron injection at NiO/dye/electrolyte interface by aluminium alkoxide treatment," *Energy & Environmental Science,* 3, 641-644, 2010.

[6] A. Morandeira, G. Boschloo, A. Hagfeldt, and L. Hammarström, "Photoinduced Ultrafast Dynamics of Coumarin 343 Sensitized p-Type-Nanostructured NiO Films," *The Journal of Physical Chemistry B,* 109, 19403-19410, 2005.

[7] P. Qin, M. Linder, T. Brinck, G. Boschloo, A. Hagfeldt, and L. Sun, "High Incident Photon-to-Current Conversion Efficiency of p-Type Dye-Sensitized Solar Cells Based on NiO and Organic Chromophores," *Advanced Materials,* 21, 2993-2996, 2009.

[8] H. Zhu, A. Hagfeldt, and G. Boschloo, "Photoelectrochemistry of Mesoporous NiO Electrodes in Iodide/Triiodide Electrolytes," *The Journal of Physical Chemistry C,* 111, 17455-17458, 2007.

[9] A. Nakasa, E. Suzuki, H. Usami, and H. Fujimatsu, "Synthesis of Porous Nickel Oxide Nanofiber," *Chemistry Letters,* 34, 428-429, 2005.

[10] A. Nattestad, X. Zhang, U. Bach, and Y.-B. Cheng, "Dye-sensitized $CuAlO_2$ photocathodes for tandem solar cell applications," *Journal of Photonics for Energy,* 1, 011103-011103-9, 2011.

[11] A. Nattestad, A. J. Mozer, M. K. R. Fischer, Y. B. Cheng, A. Mishra, P. Bauerle, and U. Bach, "Highly efficient photocathodes for dye-sensitized tandem solar cells," *Nature Materials,* 9, 31-35, 2010.

[12] E. A. Gibson, A. L. Smeigh, L. Le Pleux, J. Fortage, G. Boschloo, E. Blart, Y. Pellegrin, F. Odobel, A. Hagfeldt, and L. Hammarström, "A p-Type NiO-Based Dye-Sensitized Solar Cell with an Open-Circuit Voltage of 0.35 V," *Angewandte Chemie International Edition,* 48, 4402-4405, 2009.

[13] X.-H. Chan, J. Robert Jennings, M. Anower Hossain, K. Koh Zhen Yu, and Q. Wang, "Characteristics of p-NiO Thin Films Prepared by Spray Pyrolysis and Their Application in CdS-sensitized Photocathodes," *Journal of The Electrochemical Society,* 158, H733-H740, 2011.

[14] S. H. Kang, K. Zhu, N. R. Neale, and A. J. Frank, "Hole transport in sensitized CdS-NiO nanoparticle photocathodes," *Chemical Communications,* 47, 10419-10421, 2011.

[15] J. Velevska and M. Ristova, "Electrochromic properties of NiOx prepared by low vacuum evaporation," *Solar Energy Materials and Solar Cells,* 73, 131-139, 2002.

[16] S. Sumikura, S. Mori, S. Shimizu, H. Usami, and E. Suzuki, "Syntheses of NiO nanoporous films using nonionic triblock co-polymer templates and their application to photo-cathodes of p-type dye-sensitized solar cells," *Journal of Photochemistry and Photobiology A: Chemistry,* 199, 1-7, 2008.

[17] L. Li, E. A. Gibson, P. Qin, G. Boschloo, M. Gorlov, A. Hagfeldt, and L. Sun, "Double-Layered NiO Photocathodes for p-Type DSSCs with Record IPCE," *Advanced Materials,* 22, 1759-1762, 2010.
[18] Y. Mizoguchi and S. Fujihara, "Fabrication and Dye-Sensitized Solar Cell Performance of Nanostructured NiO/Coumarin 343 Photocathodes," *Electrochemical and Solid-State Letters,* 11, K78-K80, 2008.
[19] A. Hagfeldt, G. Boschloo, L. Sun, L. Kloo, and H. Pettersson, "Dye-Sensitized Solar Cells," *Chemical Reviews,* 110, 6595-6663, 2010.
[20] B. A. Gregg, F. Pichot, S. Ferrere, and C. L. Fields, "Interfacial Recombination Processes in Dye-Sensitized Solar Cells and Methods To Passivate the Interfaces," *The Journal of Physical Chemistry B,* 105, 1422-1429, 2001.
[21] J. R. Bolton, S. J. Strickler, and J. S. Connolly, "Limiting and realizable efficiencies of solar photolysis of water," *Nature,* 316, 495-500, 1985.
[22] A. Nakasa, H. Usami, S. Sumikura, S. Hasegawa, T. Koyama, and E. Suzuki, "A High Voltage Dye-sensitized Solar Cell using a Nanoporous NiO Photocathode," *Chemistry Letters,* 34, 500-501, 2005.
[23] Z. Ji, G. Natu, Z. Huang, and Y. Wu, "Linker effect in organic donor-acceptor dyes for p-type NiO dye sensitized solar cells," *Energy & Environmental Science,* 4, 2818-2821, 2011.
[24] D. Adler and J. Feinleib, "Electrical and Optical Properties of Narrow-Band Materials," *Physical Review B,* 2, 3112-3134, 1970.
[25] F. Safari-Alamuti, J. R. Jennings, M. A. Hossain, L. Y. L. Yung, and Q. Wang, "Conformal growth of nanocrystalline CdX (X = S, Se) on mesoscopic NiO and their photoelectrochemical properties," *Physical Chemistry Chemical Physics,* 15, 4767-4774, 2013.
[26] S. Rühle, M. Shalom, and A. Zaban, "Quantum-Dot-Sensitized Solar Cells," *ChemPhysChem,* 11, 2290-2304, 2010.
[27] I. Mora-Seró and J. Bisquert, "Breakthroughs in the Development of Semiconductor-Sensitized Solar Cells," *The Journal of Physical Chemistry Letters,* 1, 3046-3052, 2010.
[28] P. Chen, J. H. Yum, F. D. Angelis, E. Mosconi, S. Fantacci, S.-J. Moon, R. H. Baker, J. Ko, M. K. Nazeeruddin, and M. Grätzel, "High Open-Circuit Voltage Solid-State Dye-Sensitized Solar Cells with Organic Dye," *Nano Letters,* 9, 2487-2492, 2009.
[29] A. Kongkanand, K. Tvrdy, K. Takechi, M. Kuno, and P. V. Kamat, "Quantum Dot Solar Cells. Tuning Photoresponse through Size and Shape Control of CdSe−TiO2 Architecture," *Journal of the American Chemical Society,* 130, 4007-4015, 2008.
[30] A. J. Nozik, "Quantum dot solar cells," *Physica E: Low-dimensional Systems and Nanostructures,* 14, 115-120, 2002.
[31] W. W. Yu, L. Qu, W. Guo, and X. Peng, "Experimental Determination of the Extinction Coefficient of CdTe, CdSe, and CdS Nanocrystals," *Chemistry of Materials,* 15, 2854-2860, 2003.
[32] W. Shockley and H. J. Queisser, "Detailed Balance Limit of Efficiency of p-n Junction Solar Cells," *Journal of Applied Physics,* 32, 510-519, 1961.
[33] A. Franceschetti, J. M. An, and A. Zunger, "Impact Ionization Can Explain Carrier Multiplication in PbSe Quantum Dots," *Nano Letters,* 6, 2191-2195, 2006.
[34] M. T. Trinh, A. J. Houtepen, J. M. Schins, T. Hanrath, J. Piris, W. Knulst, A. P. L. M. Goossens, and L. D. A. Siebbeles, "In Spite of Recent Doubts Carrier Multiplication Does Occur in PbSe Nanocrystals," *Nano Letters,* 8, 1713-1718, 2008.
[35] G. Hodes, "Comparison of Dye- and Semiconductor-Sensitized Porous Nanocrystalline Liquid Junction Solar Cells," *The Journal of Physical Chemistry C,* 112, 17778-17787, 2008.
[36] J. H. Rhee, Y. H. Lee, P. Bera, and S. I. Seok, "Cu_2S deposited mesoporous NiO photocathode for a solar cell," *Chemical Physics Letters,* 477, 345-348, 2009.

[37] I. Hotovy, J. Huran, and L. Spiess, "Characterization of sputtered NiO films using XRD and AFM," *Journal of Materials Science,* 39, 2609-2612, 2004.
[38] M. B. Mohamed, D. Tonti, A. Al-Salman, A. Chemseddine, and M. Chergui, "Synthesis of High Quality Zinc Blende CdSe Nanocrystals," *The Journal of Physical Chemistry B,* 109, 10533-10537, 2005.
[39] M. A. Hossain, J. R. Jennings, Z. Y. Koh, and Q. Wang, "Carrier Generation and Collection in CdS/CdSe-Sensitized SnO2 Solar Cells Exhibiting Unprecedented Photocurrent Densities," *ACS Nano,* 5, 3172-3181, 2011.
[40] J. H. Bang and P. V. Kamat, "Quantum Dot Sensitized Solar Cells. A Tale of Two Semiconductor Nanocrystals: CdSe and CdTe," *ACS Nano,* 3, 1467-1476, 2009.
[41] C. Ching-Fa, L. Shih-Yi, and L. Yuh-Lang, "The heat annealing effect on the performance of CdS/CdSe-sensitized TiO 2 photoelectrodes in photochemical hydrogen generation," *Nanotechnology,* 21, 025202, 2010.
[42] U. Hotje, C. Rose, and M. Binnewies, "Lattice constants and molar volume in the system ZnS, ZnSe, CdS, CdSe," *Solid State Sciences,* 5, 1259-1262, 2003.
[43] Y.-L. Lee and Y.-S. Lo, "Highly Efficient Quantum-Dot-Sensitized Solar Cell Based on Co-Sensitization of CdS/CdSe," *Advanced Functional Materials,* 19, 604-609, 2009.
[44] J. Halme, G. Boschloo, A. Hagfeldt, and P. Lund, "Spectral Characteristics of Light Harvesting, Electron Injection, and Steady-State Charge Collection in Pressed TiO2 Dye Solar Cells," *The Journal of Physical Chemistry C,* 112, 5623-5637, 2008.
[45] P. R. F. Barnes, A. Y. Anderson, S. E. Koops, J. R. Durrant, and B. C. O'Regan, "Electron Injection Efficiency and Diffusion Length in Dye-Sensitized Solar Cells Derived from Incident Photon Conversion Efficiency Measurements," *The Journal of Physical Chemistry C,* 113, 1126-1136, 2008.
[46] J. Villanueva-Cab, H. Wang, G. Oskam, and L. M. Peter, "Electron Diffusion and Back Reaction in Dye-Sensitized Solar Cells: The Effect of Nonlinear Recombination Kinetics," *The Journal of Physical Chemistry Letters,* 1, 748-751, 2010.
[47] N. s. Guijarro, T. Lana-Villarreal, I. n. Mora-Seró, J. Bisquert, and R. Gómez, "CdSe Quantum Dot-Sensitized TiO2 Electrodes: Effect of Quantum Dot Coverage and Mode of Attachment," *The Journal of Physical Chemistry C,* 113, 4208-4214, 2009.
[48] I. Hod, V. González-Pedro, Z. Tachan, F. Fabregat-Santiago, I. Mora-Seró, J. Bisquert, and A. Zaban, "Dye versus Quantum Dots in Sensitized Solar Cells: Participation of Quantum Dot Absorber in the Recombination Process," *The Journal of Physical Chemistry Letters,* 2, 3032-3035, 2011.
[49] V. González-Pedro, X. Xu, I. Mora-Seró, and J. Bisquert, "Modeling High-Efficiency Quantum Dot Sensitized Solar Cells," *ACS Nano,* 4, 5783-5790, 2010.
[50] S. Giménez, I. Mora-Seró, L. Macor, N. Guijarro, T. Lana-Villarreal, R. Gómez, L. J. Diguna, Q. Shen, T. Toyoda, and J. Bisquert, "Improving the performance of colloidal quantum-dot-sensitized solar cells," *Nanotechnology,* 20, 295204, 2009.
[51] H. J. Lee, J. Bang, J. Park, S. Kim, and S.-M. Park, "Multilayered Semiconductor (CdS/CdSe/ZnS)-Sensitized TiO2 Mesoporous Solar Cells: All Prepared by Successive Ionic Layer Adsorption and Reaction Processes," *Chemistry of Materials,* 22, 5636-5643, 2010/10/12 2010.
[52] R. Vogel, K. Pohl, and H. Weller, "Sensitization of highly porous, polycrystalline TiO2 electrodes by quantum sized CdS," *Chemical Physics Letters,* 174, 241-246, 1990.
[53] P. Sudhagar, V. Gonzalez-Pedro, I. Mora-Sero, F. Fabregat-Santiago, J. Bisquert, and Y. S. Kang, "Interfacial engineering of quantum dot-sensitized TiO2 fibrous electrodes for futuristic photoanodes in photovoltaic applications," *Journal of Materials Chemistry,* 22, 14228-14235, 2012.

[54] J. G. Radich, R. Dwyer, and P. V. Kamat, "Cu2S Reduced Graphene Oxide Composite for High-Efficiency Quantum Dot Solar Cells. Overcoming the Redox Limitations of S2−/Sn2− at the Counter Electrode," *The Journal of Physical Chemistry Letters*, 2, 2453-2460, 2011.

[55] I. Mora-Seró and J. Bisquert, "Impedance characterization of Quantum Dot Sensitized Solar Cells."

[56] P. Reiss, M. Protière, and L. Li, "Core/Shell Semiconductor Nanocrystals," *Small*, 5, 154-168, 2009.

[57] S. S. Lo, T. Mirkovic, C.-H. Chuang, C. Burda, and G. D. Scholes, "Emergent Properties Resulting from Type-II Band Alignment in Semiconductor Nanoheterostructures," *Advanced Materials*, 23, 180-197, 2011.

[58] C.-F. Chi, H.-W. Cho, H. Teng, C.-Y. Chuang, Y.-M. Chang, Y.-J. Hsu, and Y.-L. Lee, "Energy level alignment, electron injection, and charge recombination characteristics in CdS/CdSe cosensitized TiO[sub 2] photoelectrode," *Applied Physics Letters*, 98, 012101, 2011.

[59] H. Gerischer, "Neglected problems in the pH dependence of the flatband potential of semiconducting oxides and semiconductors covered with oxide layers," *Electrochimica Acta*, 34, 1005-1009, 1989.

[60] D. V. Talapin, I. Mekis, S. Götzinger, A. Kornowski, O. Benson, and H. Weller, "CdSe/CdS/ZnS and CdSe/ZnSe/ZnS Core−Shell−Shell Nanocrystals," *The Journal of Physical Chemistry B*, 108, 18826-18831, 2004.

[61] C. Trager-Cowan, P. Parbrook, B. Henderson, and K. O'Donnell, "Band alignments in Zn (Cd) S (Se) strained layer superlattices," *Semiconductor Science and Technology*, 7, 536, 1999.

[62] A. M. Smith and S. Nie, "Semiconductor Nanocrystals: Structure, Properties, and Band Gap Engineering," *Accounts of Chemical Research*, 43, 190-200, 2009.

[63] A. Zaban, M. Greenshtein, and J. Bisquert, "Determination of the Electron Lifetime in Nanocrystalline Dye Solar Cells by Open-Circuit Voltage Decay Measurements," *ChemPhysChem*, 4, 859-864, 2003.